Effects of vacancy transport and surface adsorption on grain boundary migration in pure metals

Alexander F. Chadwick [*] and Peter W. Voorhees [†]
Department of Materials Science and Engineering, Northwestern University, 2220 Campus Drive, Evanston, Illinois 60208, USA

(Received 5 December 2023; accepted 13 February 2024; published 27 February 2024)

Vacancy transport has a demonstrable impact on the microstructural evolution of polycrystalline metals, but existing models typically require knowledge of the stress state in order to describe lattice site generation and annihilation at interfaces. Using irreversible thermodynamics, the driving forces and equilibrium conditions dictating the response of incoherent interfaces are derived for a pure metal with vacancies under stress-free conditions. A phenomenological set of linear kinetic expressions that guarantees a decrease in the total energy upon diffusion is proposed. A near-equilibrium steady-state analytical solution for grain boundaries is obtained. In the stress-free limit, interface migration and transboundary diffusion are closely coupled, as are the production or annihilation of vacancies and the rigid-body dilation or contraction of the bulk grains. Solutions for various limiting kinetic regimes are also obtained, and the relevance of the kinetic parameters to pore nucleation at grain boundaries is discussed.

DOI: 10.1103/PhysRevMaterials.8.023602

I. INTRODUCTION

Vacancies have long been known to affect the time-dependent microstructural evolution of crystalline materials. Vacancy transport and reaction kinetics strongly affect certain regimes of creep [1–9], the sintering of porous materials [10–17], and grain growth [6,9,13,18], to name a few scenarios. Additionally, vacancies can interact with alloying elements to produce solute trapping [19]. These kinetic effects are exaggerated by the length scales of the system; for example, increased vacancy transport strongly affects the evolution of nanocrystalline materials [20,21], and the initial diameter of Ni-Ti microwires determines whether Kirkendall pores that form during interdiffusion will either coalesce into a central channel or remain widely distributed throughout the wire [22]. The vacancies may be generated by various processes, such as irradiation [15,19,23–26], imbalanced interdiffusion (i.e., the Kirkendall effect) [22,27–31], or simply by the motion of interfaces between crystals [12,13,32–36].

Due to their influence on the overall evolution of the system, it is therefore desirable to understand the implications of how vacancies interact with interfaces in crystalline materials at the continuum scale, whether they be free surfaces (i.e., at pores and voids), grain boundaries, or phase boundaries. Such a theory would then describe how these interfaces move in conjunction with bulk transport of vacancies and other species, as well as other phenomena. Examples of this approach have previously been presented in the literature. Larché and Cahn applied classical thermodynamics to derive the equilibrium conditions at a solid-fluid interface for a rigid network lattice in both linear and nonlinear regimes [37,38]. They subsequently extended this approach to solid-solid interfaces [39]. For these regimes, they found that the interface was stationary when each side had the same grand potential density, that the concentration field was at equilibrium when the diffusion potentials were uniform, and that the system had to be in global mechanical equilibrium. Later [40], Larché and Cahn employed an irreversible thermodynamic formulation of the previous models to obtain the kinetics by which the previous examples evolved towards equilibrium and rigorously derived an improved version of Herring's analysis of vacancy-mediated diffusional creep [2]. A pedagogical review of this approach is given in [41].

An important consequence of the network lattice in the Larché and Cahn models is that a nonzero vacancy chemical potential is only a definable quantity at certain line defects (e.g., dislocations) or interfaces under hydrostatic stress states; therefore, particular care must be taken when constructing the thermodynamic potentials of the system. Mishin *et al.* derived a generalized framework from irreversible thermodynamics to describe diffusional creep that considered both classical and nonclassical (i.e., gradient) terms in the driving forces [4]. While this model is able to relax the network lattice constraint, it is challenging to employ in computations. Thus, Mishin *et al.* subsequently derived a sharp-interface model that, like their previous model, found that the grand potential was the primary driving force for interface migration and lattice site generation and annihilation at the interface [5]. Numerical and transient analytical solutions of this latter model have recently been presented by McFadden *et al.* [6]. Cermelli and Gurtin also derived a general theory for the kinetics of incoherent interfaces from irreversible thermodynamics that included the effects of stress and configurational forces in the interface, but required that species were in local equilibrium at the interface [35]. The work of Svoboda, Fischer, and collaborators used the thermodynamic extremal principle to derive

[*]Present Address: U.S. Naval Research Laboratory, 4555 Overlook Avenue SW, Washington, DC 20375; alexander.chadwick@nrl.navy.mil
[†]p-voorhees@northwestern.edu

kinetic models for lattice site generation and annihilation at line defects in the presence of stress [7,8]. In these models, the driving force for the lattice site reaction is a generalized vacancy chemical potential tensor that should be roughly equivalent to the grand potential of the previous models under hydrostatic conditions. The derived model was subsequently applied to study the Kirkendall effect (bulk material flow during interdiffusion of materials with mismatched diffusion coefficients) and predict the possibility of Kirkendall porosity formation near interfaces in Cu-Sn intermetallic compounds [27]. Various models of vacancy and interface interactions at the atomistic scale have also been investigated [9,34,36,42].

While the previous continuum models are general in nature and should therefore be broadly applicable, the inclusion of nonhydrostatic stress states can make the resulting formulations complex and computationally intensive [4]. Thus, it would be worthwhile to derive the nonequilibrium thermodynamics and kinetics of vacancy and interface interactions in the absence of stress to understand how vacancy transport affects interface motion and the resulting microstructural evolution. One such set of kinetics was derived for voids in irradiated Cu by Hochrainer and El-Azab [23]. In that model, they investigated the activation barriers for the lattice site annihilation reaction and the resulting interface velocity, as well as the deviations of the vacancy and interstitial concentrations from the equilibrium Gibbs-Thomson condition. A subsequent asymptotic analysis by Ahmed and El-Azab found that typical Hohenberg-Halperin Model C phase-field formulations can readily capture the nonequilibrium stress-free kinetics at void surfaces [43]. Several other phase-field and smoothed-boundary methods have also been proposed to examine various vacancy and interface interactions [14–17,24,25,30,31]. The difference between many of these models is whether vacancy sinks are source terms at free surfaces [24,25,43], source terms at grain boundaries that cause rigid-body motion [14,16,17], or if they are distributed throughout the bulk of the crystal to produce variations in the local lattice dilation rate [30,31]. Vacancies are thus removed from the solid through an explicit reaction at interfaces or defects. By comparison, the model of Greenquist *et al.* assumes that grain boundaries provide enhanced vacancy diffusion to the free surface, where the mobility is chosen to produce local equilibrium of the vacancy concentration [15]. Therefore, any vacancy production or annihilation reaction is assumed to have ideally fast kinetics.

In addition to the work of Hochrainer and El-Azab [23], a series of sharp-interface models were previously derived by Estrin, Lücke, and Gottstein [32,33,44]. These models constructed a set of moving-reference-frame expressions for the vacancy concentration profile in the vicinity of a moving grain boundary and introduced a vacancy drag correction to a generalized driving force for interface motion. As desired in this work, these models do not require knowledge of the stress state in order to be solvable. However, the derivation of these earlier models is phenomenological in nature. McFadden *et al.* demonstrate that the sharp-interface model of Mishin *et al.* may be simplified to a low-strain-rate regime where the elastic stress in the bulk of a crystal vanishes [5,6]. However, the lattice velocities in the model of Mishin *et al.* act to dissipate mechanical stress within the bulk of a grain, and lattice site creation at the grain boundary produces a local deformation that is eventually accommodated by this bulk lattice flow [5]. Therefore, McFadden *et al.* introduce an assumption of rigid-body motion in order to solve the velocity profile within each grain [6].

In this work, we therefore derive the overall energy dissipation rate at free surfaces and solid-solid interfaces in the stress-free limit. We follow a similar approach to Mishin *et al.* [5], but we assume rigid-body motion as in McFadden *et al.* [6]. This allows for facile inclusion of lattice site generation and annihilation reactions in the stress-free regime, although the present derivation is limited to planar interfaces. Additionally, we relax the assumption of constant excess Helmholtz free energy at the interface employed in Refs. [5,6] and explicitly include the composition of the interface and its resulting influence on the overall dissipation. We also do not assume local chemical equilibrium, in contrast to Cermelli and Gurtin [35]. After deriving the dissipation rate, we apply the principles of irreversible thermodynamics to obtain a phenomenological set of linear kinetic expressions describing the evolution of the interfaces. Lastly, we obtain a set of approximate analytical solutions for the steady-state response of the interface to a set of applied bulk fluxes and examine limiting values and simplifying regimes of the obtained solution for the grain boundary response.

II. THEORY

In this section, we derive an irreversible thermodynamic model of a metal comprised of one element and vacancies and obtain the equilibrium conditions of the system and the driving forces for the evolution of planar grain and phase boundaries. In general, the model derivation is similar to the approach of Mishin *et al.* [5], but several additional key assumptions are employed for this work. The assumptions are as follows:

(1) All interfaces are planar with no curvature. Additionally, there are no gradients in any quantities along directions tangential to the interfaces.

(2) The system is at a sufficient temperature such that all stresses are fully relaxed, i.e., it is stress free.

(3) Within a phase, all species have equal partial molar volumes.

(4) If necessary, grains may translate relative to each other by rigid-body motion.

(5) Dislocations that may climb by absorption or emission of vacancies are present at solid-solid interfaces such that these boundaries can create or annihilate lattice sites.

(6) Solid-solid interfaces are incoherent; thus, there is no misfit strain.

Assumptions 1–4 simplify the resulting model as they eliminate the plastic deformation that is present in Refs. [5,35]. Additionally, assumption 3 leads to a network lattice constraint in the bulk crystals away from interfaces. However, the inclusion of assumption 4 allows the model to be applicable to both grain boundaries in polycrystalline single-phase materials and allotropic phase boundaries that differ in their equilibrium lattice site density. When there is a jump in the lattice site density across the incoherent interface, the mismatch may be accommodated by the rigid-body motion of

the phases. In general, assumptions 1–4 may not be needed in order to derive a stress-free model. However, in more than one dimension the resulting rigid-body motion introduces significant complexity to both thermodynamic and numerical models and is not necessarily well posed [28–30,45,46]. Assumptions 4–6 are necessary to allow the model to consider lattice site generation and annihilation at solid-solid interfaces; in Ref. [5], these processes were solely due to the elastic effects that have been neglected.

We begin with a few preliminary definitions. The Helmholtz free energy density of the bulk solid is

$$f^b = f^b(T, \rho_A), \tag{1}$$

where f^b is the Helmholtz free energy per unit volume, T is temperature, and ρ_A is the number density of A atoms [41]. The number density of vacancies ρ_V can be calculated by the relationship

$$\rho_A + \rho_V = \rho_0, \tag{2}$$

where ρ_0 is the nominal lattice site density. As in Mishin *et al.* [5], we assume that the solid is comprised of a primitive Bravais lattice such that the equivalence of different lattice site configurations can be neglected. Assuming that the system is isothermal, closed, and stress free, Eq. (1) is [41]

$$f^b = M^b \rho_A + \mu_V^b \rho_0, \tag{3}$$

where M^b is the diffusion potential of atoms with respect to vacancies and μ_V^b is the chemical potential of vacancies or vacancy chemical potential. The values of M^b and μ_V^b are related by

$$M^b = \mu_A^b - \mu_V^b, \tag{4}$$

where μ_A^b is the chemical potential of atoms. In Eq. (3), M^b arises variationally as a local Lagrange multiplier that relates the change in f^b to a change in ρ_A for a fixed number density of lattice sites [40,41]. Likewise, μ_V^b is a local Lagrange multiplier that relates the change in f^b to a change in ρ_V for a fixed number density of atoms. The vacancy chemical potential μ_V^b is only definable due to the lack of shear stresses in the system, which is not the case in Ref. [5]. The first variation of Eq. (3) is [41]

$$\delta f^b = M^b \delta \rho_A, \tag{5}$$

as ρ_0 is fixed in the bulk phase. Lastly, the assumption of a network lattice leads to a constraint on the bulk fluxes of each species:

$$\mathbf{J}_V^b + \mathbf{J}_A^b = 0, \tag{6}$$

where $\mathbf{J}_A^b$ is the bulk flux of atoms and $\mathbf{J}_V^b$ is the bulk flux of vacancies.

In this work, we explicitly consider the composition of the interface. The interface, whether a free surface or a solid-solid boundary, is treated as a Gibbs dividing surface with associated excess quantities of the energies, potentials, and densities [47]. Here,

$$f^\Sigma = f^\Sigma(T, \Gamma_A, \Gamma_V, \gamma) \tag{7}$$

is the excess Helmholtz free energy per unit area of the dividing surface, where Γ_A and Γ_V are the excess number densities per unit area of atoms and vacancies, respectively, and γ is the interfacial energy. While it is possible for the excess surface density of lattice sites ($\Gamma_0 = \Gamma_A + \Gamma_V$) to vary at grain boundaries, this may introduce an excess stress to the interface that must then be accommodated [36]. As we have assumed a negligible stress state in the system (assumption 2), we shall also assume that Γ_0 is a constant. This assumption also leads to well-defined values of the equilibrium chemical potentials [48,49]. Therefore, for fixed Γ_0 in a planar, isothermal system, the first variation of f^Σ is assumed to be

$$\delta f^\Sigma = M^\Sigma \delta \Gamma_A, \tag{8}$$

where M^Σ is the excess diffusion potential of atoms. The variation of f^Σ with respect to γ vanishes due to the assumption of a planar interface. As we have introduced the composition dependence of the interface into the model, we must also derive corresponding modifications to the generalized transport laws of the system [46]. These are detailed as needed in the following sections and the Appendixes.

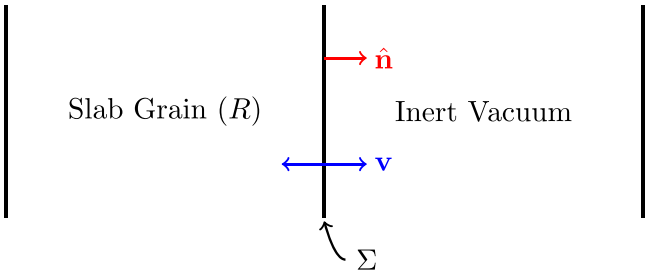

FIG. 1. A schematic of the system considered in Sec. II A, comprised of a semi-infinite slab (R) with a single planar dividing surface (Σ) exposed to a vacuum. The location of Σ, the outward unit normal, and the velocity vector are marked.

A. Behavior of free surfaces

While this work focuses on the response of grain and phase boundaries, we first consider the irreversible thermodynamics of a system comprised of a slab of material with one planar Gibbsian free surface exposed to vacuum. This allows for better insight into the thermodynamics of the solid-solid interface, as the associated derivations for each domain contain similar terms. A schematic depiction of this example is given in Fig. 1. For such a system, the total free energy Φ is

$$\Phi = \int_R f^b dV + \int_\Sigma f^\Sigma dA, \tag{9}$$

where R denotes the slab and Σ denotes the Gibbsian free surface. Following Refs. [5,41,46], the total rate at which energy is dissipated in this system, $\dot{\Phi}$, can be expressed as

$$\begin{aligned}\dot{\Phi} &= \frac{d}{dt}\int_R f^b dV + \frac{d}{dt}\int_\Sigma f^\Sigma dA \\ &= \int_R \frac{\partial f^b}{\partial t} dV + \int_\Sigma \frac{\partial f^\Sigma}{\partial t} dA + \int_\Sigma f^b \hat{\mathbf{n}} \cdot \mathbf{v}\, dA,\end{aligned} \tag{10}$$

where the second line arises after applying Reynolds' theorem. Here, t is time, $\hat{\mathbf{n}}$ is the outward unit normal vector that points from the solid to the vacuum, and $\mathbf{v}$ is the velocity of

the free surface in the laboratory frame. The first integral, which corresponds to the rate of dissipation in the bulk of the grain, arises due to the transport of species within the grain. The second integral, which corresponds to dissipation on the surface, arises due to adsorption or transport of species to the surface. The third integral, which corresponds to the rate of dissipation at the surface of the slab due to the moving boundary, arises from the accretion of lattice sites.

By Eqs. (5) and (8), $\dot{\Phi}$ becomes

$$\dot{\Phi} = \int_R M^b \frac{\partial \rho_A}{\partial t} dV + \int_\Sigma M^\Sigma \frac{\partial \Gamma_A}{\partial t} dA + \int_\Sigma f^b \hat{\mathbf{n}} \cdot \mathbf{v}\, dA. \quad (11)$$

The time derivative of the bulk concentration is assumed to obey the continuity equation

$$\frac{\partial \rho_A}{\partial t} = -\nabla \cdot \mathbf{J}_A^b. \quad (12)$$

Per our model assumptions, the interface is planar with uniform values of surface quantities; therefore, for the evolution of the surface concentration, we employ a continuity equation of the form [41,50]

$$\frac{\partial \Gamma_A}{\partial t} = -j_A^T, \quad (13)$$

where j_A^T is a transverse adsorption flux of atoms from the surface. Inserting Eqs. (12) and (13), Eq. (11) becomes

$$\dot{\Phi} = -\int_R M^b \nabla \cdot \mathbf{J}_A^b dV - \int_\Sigma M^\Sigma j_A^T dA + \int_\Sigma f^b \hat{\mathbf{n}} \cdot \mathbf{v}\, dA. \quad (14)$$

Next, we apply the divergence theorem to the first integral of Eq. (14). If we assume that Σ is the only active surface, we obtain

$$\dot{\Phi} = \int_R \mathbf{J}_A^b \cdot \nabla M^b dV - \int_\Sigma M^b \hat{\mathbf{n}} \cdot \mathbf{J}_A^b dA - \int_\Sigma M^\Sigma j_A^T dA + \int_\Sigma f^b \hat{\mathbf{n}} \cdot \mathbf{v}\, dA, \quad (15)$$

where the second integral represents the boundary conditions for bulk diffusion at the free surface.

To complete the derivation, we introduce expressions to capture the overall mass balance at the free surface [5,51]:

$$\hat{\mathbf{n}} \cdot \mathbf{J}_A^b = -q_A^b + \rho_A \hat{\mathbf{n}} \cdot \mathbf{v}, \quad (16)$$

$$j_A^T = -q_A^\Sigma, \quad (17)$$

where q_A^b and q_A^Σ are scalar adsorption fluxes that are positive when atoms are added to the bulk or surface and negative when removed. Additionally, the overall balance of vacancies in the system leads to the surface condition

$$H_V^\Sigma = \rho_0 \hat{\mathbf{n}} \cdot \mathbf{v}, \quad (18)$$

where H_V^Σ is a vacancy generation and annihilation rate in the interface that is positive when vacancies are created and negative when they are destroyed. Thus, the motion of the surface requires that vacancies be created or destroyed at the free surface. The derivation of Eqs. (16)–(18) is presented in Appendix A. As described in Appendix A, the total number of atoms is conserved, and therefore

$$q_A^b + q_A^\Sigma = 0. \quad (19)$$

However, vacancies may be generated or annihilated as needed, and therefore H_V^Σ can be nonzero. We may now begin simplifying Eq. (10) by inserting Eqs. (11)–(18). Doing so, we eventually obtain[1]

$$\dot{\Phi} = \int_R \mathbf{J}_A^b \cdot \nabla M^b dV + \int_\Sigma (M^b - M^\Sigma) q_A^b dA + \int_\Sigma \omega \hat{\mathbf{n}} \cdot \mathbf{v}\, dA, \quad (20)$$

where

$$\omega = f^b - \rho_A M^b = \rho_0 \mu_V^b \quad (21)$$

is the grand potential density in the bulk [5,41]. Thus, the value of the grand potential is related to the vacancy chemical potential.

By inspection of Eq. (20), there are three conditions dictating the global thermodynamic equilibrium of the slab that correspond to each set of integrals. These conditions and the phenomena that occur if they are violated are as follows:

(1) $\nabla M^b = 0$, or there will be bulk diffusion of atoms within the slab.

(2) $M^b = M^\Sigma$, or there will be an adsorptive flux of atoms between the bulk and surface phases, depending upon the relative difference in potentials.

(3) $\omega = 0$, or the surface will migrate by creating or destroying vacancies.

If any of these conditions are not satisfied, then the free surface evolves to dissipate energy. The first and third integrals of Eq. (20) and their corresponding effects are generally equivalent to Eq. (45) in Ref. [5] in the absence of elastic effects and adsorption. The second integral arises from the presence of a varying f^Σ in the present model. Equation (20) and conditions 1–3 also agree with previously derived equilibrium conditions derived for the free surface [38,40,41].

B. Behavior of solid-solid interfaces

We now consider the behavior of a general solid-solid interface. The derivation should be equally applicable to grain boundaries and phase boundaries, provided the general assumptions of the model are satisfied. Here, the system is composed of two semi-infinite slab grains α and β, with associated domains R^α and R^β, as depicted in Fig. 2. The grains are separated by an interface or dividing surface Σ, and each grain is partially enclosed by an outer inert surface S^α and S^β, respectively. We assume that Σ may act as a source or sink of lattice sites by generating or annihilating vacancies. Therefore, the total volume of the system is not fixed (i.e., the system will dilate or contract as lattice sites are produced or destroyed), and rigid-body motion must be introduced to the model to accommodate the relative translation of β with respect to α, or vice versa. As will be discussed later, the

[1]We note that we can equivalently choose j_A^T or q_A^Σ to represent the fluxes at the surface in Eq. (20); the present choice is made for parallelism with the solid-solid interface behavior that is derived later in this work.

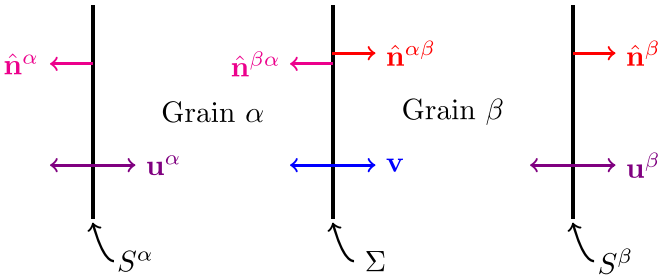

FIG. 2. A schematic of the system employed in Sec. II B, comprised of two grains α and β and a planar dividing surface Σ. Each grain also has its own inert bounding surface S^{α} and S^{β}. The grains Σ, S^{α}, and S^{β}, the velocities, and the outward normal vectors at each interface are all marked.

location of either Σ, S^{α}, or S^{β} may be fixed in the laboratory reference frame, but the particular choice does not necessarily matter.

There is a contact boundary condition between α and β; thus, $\hat{\mathbf{n}}^{\alpha\beta} = -\hat{\mathbf{n}}^{\beta\alpha}$, where $\hat{\mathbf{n}}^{\alpha\beta}$ is the outward unit normal vector pointing from α to β and $\hat{\mathbf{n}}^{\beta\alpha}$ is the outward unit normal vector pointing from β to α. Additionally, we assume that S^{α} and S^{β} are both parallel to Σ such that $\hat{\mathbf{n}}^{\alpha\beta} = -\hat{\mathbf{n}}^{\alpha} = \hat{\mathbf{n}}^{\beta}$, where $\hat{\mathbf{n}}^{\alpha}$ is the outward unit normal vector pointing from α to outside the system and $\hat{\mathbf{n}}^{\beta}$ is the outward unit normal vector pointing from β to outside the system. In the subsequent derivations, many terms depend on average values and differences of a quantity between the two bulk phases. For simplicity, we denote the average value of a quantity ψ between bulk phases as

$$\langle\psi\rangle = (\psi^{\alpha} + \psi^{\beta})/2 \tag{22}$$

and the difference or jump as

$$[\![\psi]\!] = \psi^{\alpha} - \psi^{\beta}. \tag{23}$$

These identities also hold for vector quantities.

As in Sec. II A, the goal is to obtain the total rate at which free energy is dissipated from the system. The analog to Eq. (9) for the two-grain system is

$$\begin{aligned}\Phi &= \Phi^{\alpha} + \Phi^{\beta} + \Phi^{\Sigma} \\ &= \int_{R^{\alpha}} f^{\alpha} dV + \int_{R^{\beta}} f^{\beta} dV + \int_{\Sigma} f^{\Sigma} dA,\end{aligned} \tag{24}$$

where Φ^{α} and Φ^{β} are the energies contributed by each grain, which are associated with their respective bulk Helmholtz energy densities f^{α} and f^{β}, and Φ^{Σ} is the energy contributed by the interface with excess areal Helmholtz energy density f^{Σ} defined by Eq. (7) and associated variation (8).

We proceed by applying the generalized transport laws derived in Appendix B. Applying Eq. (B11) to (24) yields

$$\begin{aligned}\dot{\Phi} = &\int_{R^{\alpha}} \frac{Df^{\alpha}}{Dt} dV + \int_{R^{\beta}} \frac{Df^{\beta}}{Dt} dV + \int_{\Sigma} \frac{\partial f^{\Sigma}}{\partial t} dA \\ &+ \int_{\Sigma} [\![f]\!]\mathbf{n}^{\alpha\beta} \cdot (\mathbf{v} - \langle\mathbf{u}\rangle) dA - \int_{\Sigma} \langle f\rangle \mathbf{n}^{\alpha\beta} \cdot [\![\mathbf{u}]\!] dA.\end{aligned} \tag{25}$$

Here, D/Dt indicates the material derivative in the moving reference of the corresponding grain, $\mathbf{v}$ is the velocity of the grain boundary, and $\mathbf{u}^{\alpha}$ and $\mathbf{u}^{\beta}$ are the velocities of S^{α} and S^{β}, respectively. Due to the assumption of rigid-body motion, $\mathbf{u}^{\alpha}$ and $\mathbf{u}^{\beta}$ also indicate the translation velocity of the bulk lattice in each grain. The quantity $\mathbf{v} - \langle\mathbf{u}\rangle$ indicates the migration of the grain boundary relative to the average translation of the bulk lattices, and $[\![\mathbf{u}]\!]$ indicates the dilation or contraction of the system. The temporal derivatives in the first three integrals may be obtained from substituting the relevant variations of the Helmholtz energy densities, Eqs. (5) and (8). Simultaneously, we adopt continuity equations of the form

$$\frac{D\rho_A^{\zeta}}{Dt} = -\nabla \cdot \mathbf{J}_A^{\zeta} \tag{26}$$

for the bulk concentrations, where $\mathbf{J}_A^{\zeta}$ is the bulk flux of A in ζ, and Eq. (13) for the surface concentrations. Therefore, Eq. (25) becomes

$$\begin{aligned}\dot{\Phi} = &-\int_{R^{\alpha}} M^{\alpha} \nabla \cdot \mathbf{J}_A^{\alpha} dV - \int_{R^{\beta}} M^{\beta} \nabla \cdot \mathbf{J}_A^{\beta} dV \\ &- \int_{\Sigma} M^{\Sigma} j_A^T dA + \int_{\Sigma} [\![f]\!]\mathbf{n}^{\alpha\beta} \cdot (\mathbf{v} - \langle\mathbf{u}\rangle) dA \\ &- \int_{\Sigma} \langle f\rangle \mathbf{n}^{\alpha\beta} \cdot [\![\mathbf{u}]\!] dA.\end{aligned} \tag{27}$$

We may apply vector calculus identities and the divergence theorem to the first two integrals, which yields

$$\begin{aligned}\dot{\Phi} = &\int_{R^{\alpha}} \mathbf{J}_A^{\alpha} \cdot \nabla M^{\alpha} dV + \int_{R^{\beta}} \mathbf{J}_A^{\beta} \cdot \nabla M^{\beta} dV \\ &- \int_{\Sigma} M^{\alpha} \mathbf{n}^{\alpha\beta} \cdot \mathbf{J}_A^{\alpha} dA + \int_{\Sigma} M^{\beta} \mathbf{n}^{\alpha\beta} \cdot \mathbf{J}_A^{\beta} dA \\ &- \int_{\Sigma} M^{\Sigma} j_A^T dA + \int_{\Sigma} [\![f_b]\!]\mathbf{n}^{\alpha\beta} \cdot (\mathbf{v} - \langle\mathbf{u}\rangle) dA \\ &- \int_{\Sigma} \langle f_b\rangle \mathbf{n}^{\alpha\beta} \cdot [\![\mathbf{u}]\!] dA.\end{aligned} \tag{28}$$

As in Sec. II A, further simplification of Eq. (28) requires the incorporation of the mass balance conditions at the grain boundary, which are derived in Appendix C. For atoms, we obtain the set of conditions at the solid-solid interface,

$$q_A^{\alpha} = -\mathbf{n}^{\alpha\beta} \cdot \mathbf{J}_A^{\alpha} + \rho_A^{\alpha} \mathbf{n}^{\alpha\beta} \cdot (\mathbf{v} - \mathbf{u}^{\alpha}), \tag{29}$$

$$q_A^{\beta} = \mathbf{n}^{\alpha\beta} \cdot \mathbf{J}_A^{\beta} - \rho_A^{\beta} \mathbf{n}^{\alpha\beta} \cdot (\mathbf{v} - \mathbf{u}^{\beta}), \tag{30}$$

$$q_A^{\Sigma} = -j_A^T, \tag{31}$$

where each q_A^{ζ} is a scalar adsorption flux of atoms that is positive when atoms are added to region ζ and negative when removed [5,51]. In a closed, isolated system, the total number of atoms is conserved and, therefore,

$$q_A^{\alpha} + q_A^{\beta} + q_A^{\Sigma} = 0. \tag{32}$$

A similar set of fluxes and interface conditions exist for vacancies; as in Sec. II A vacancies are not conserved, leading to a production rate of vacancies at the interface H_V^{Σ}. As derived in Appendix C, we eventually obtain the constraint

$$H_V^{\Sigma} = [\![\rho_0]\!]\mathbf{n}^{\alpha\beta} \cdot (\mathbf{v} - \langle\mathbf{u}\rangle) - \langle\rho_0\rangle \mathbf{n}^{\alpha\beta} \cdot [\![\mathbf{u}]\!], \tag{33}$$

where ρ_0^ζ is the bulk lattice site density in the corresponding phase. Equation (33) dictates the relationship between the vacancy production rate, the interface migration, and the dilation or contraction of the system. We may now begin to simplify Eq. (28); by combining it with Eqs. (29)–(33), we obtain

$$\begin{aligned}\dot{\Phi} = &\int_{R^\alpha} \mathbf{J}_A^\alpha \cdot \nabla M^\alpha dV + \int_{R^\beta} \mathbf{J}_A^\beta \cdot \nabla M^\beta dV \\ &+ \int_\Sigma \left(q_A^\alpha M^\alpha + q_A^\beta M^\beta + q_A^\Sigma M^\Sigma\right) dA \\ &+ \int_\Sigma (\llbracket f_b \rrbracket - \llbracket M\rho_A \rrbracket)\mathbf{n}^{\alpha\beta} \cdot (\mathbf{v} - \langle \mathbf{u} \rangle) dA \\ &- \int_\Sigma (\langle f_b \rangle - \langle M\rho_A \rangle)\mathbf{n}^{\alpha\beta} \cdot \llbracket \mathbf{u} \rrbracket dA. \end{aligned} \tag{34}$$

After further simplification, we finally obtain

$$\begin{aligned}\dot{\Phi} = &\int_{R^\alpha} \mathbf{J}_A^\alpha \cdot \nabla M^\alpha dV + \int_{R^\beta} \mathbf{J}_A^\beta \cdot \nabla M^\beta dV \\ &+ \int_\Sigma \left(q_A^\alpha (M^\alpha - M^\Sigma) + q_A^\beta (M^\beta - M^\Sigma)\right) dA \\ &+ \int_\Sigma \llbracket \omega \rrbracket \mathbf{n}^{\alpha\beta} \cdot (\mathbf{v} - \langle \mathbf{u} \rangle) dA - \int_\Sigma \langle \omega \rangle \mathbf{n}^{\alpha\beta} \cdot \llbracket \mathbf{u} \rrbracket dA. \end{aligned} \tag{35}$$

Here, we have employed Eq. (32) to eliminate q_A^Σ from the dissipation rate. The bulk grand potential densities ω^α and ω^β are defined equivalently to Eq. (21).

In the simplified overall dissipation rate, there are multiple processes that act to equilibrate the system, leading to a total of six conditions that must be satisfied to ensure equilibrium:

(1) $\nabla M^\alpha = 0$, or bulk diffusion occurs in grain α.
(2) $\nabla M^\beta = 0$, or bulk diffusion occurs in grain β.
(3) $M^\alpha = M^\Sigma$, or atoms adsorb at the interface from α.
(4) $M^\beta = M^\Sigma$, or atoms adsorb at the interface from β.
(5) $\llbracket \omega \rrbracket = 0$, or the interface will migrate.
(6) $\langle \omega \rangle = 0$, or the system will dilate or contract.

Depending upon the values of $\llbracket \rho_0 \rrbracket$ and $\langle \rho_0 \rangle$, the final two conditions may also imply a nonzero H_V^Σ. Conditions 1 and 2 are consistent with the previous model of Mishin *et al.* [5]. Additionally, if q_A^α and q_A^β are equal and opposed, the dependence upon M^Σ vanishes from (35) and the resulting equilibrium condition of $M^\alpha = M^\beta$ is equivalent to the one for transboundary diffusion in Mishin *et al.* [5]. The largest difference in this work arises from conditions 5 and 6, which govern the lattice site generation or annihilation, the interface migration, and the dilation or contraction of the system. In this work, each of these processes has a unique equilibrium condition due to the stress-free assumption and the introduction of variable surface concentrations. However, due to Eq. (32), either migration, dilation, or contraction in the system requires that vacancies be generated or annihilated. By comparison, in Mishin *et al.* the corresponding lattice site generation or annihilation process was only linked with lattice translation, which itself was due to mechanical effects in the system [5]. Additionally, as we have assumed planar interfaces to ensure the solvability of the rigid-body motion, no contributions from curvature exist in the present driving forces or equilibrium conditions. The existence of conditions 5 and 6 is consistent with the work of Larché and Cahn [37–40] and Voorhees and Johnson [41], who argued that, at incoherent boundaries or in the presence of climbable dislocations, the interface should act to equilibrate the vacancy chemical potential. This may be demonstrated by recognizing that $\llbracket \omega \rrbracket = \llbracket \rho_0 \mu_V \rrbracket$ and $\langle \omega \rangle = \langle \rho_0 \mu_V \rangle$. If we explicitly include H_V^Σ through Eq. (33), the final two terms of Eq. (35) may be equivalently written as

$$\begin{aligned}&\int_\Sigma \llbracket \omega \rrbracket \mathbf{n}^{\alpha\beta} \cdot (\mathbf{v} - \langle \mathbf{u} \rangle) dA - \int_\Sigma \langle \omega \rangle \mathbf{n}^{\alpha\beta} \cdot \llbracket \mathbf{u} \rrbracket dA \\ &\quad = \int_\Sigma \langle \mu_V \rangle H_V^\Sigma dA + \int_\Sigma \langle \rho_0 \rangle \llbracket \mu_V \rrbracket \mathbf{n}^{\alpha\beta} \cdot (\mathbf{v} - \langle \mathbf{u} \rangle) dA \\ &\qquad - \frac{1}{4} \int_\Sigma \llbracket \rho_0 \rrbracket \llbracket \mu_V \rrbracket \mathbf{n}^{\alpha\beta} \cdot \llbracket \mathbf{u} \rrbracket dA. \end{aligned} \tag{36}$$

Thus, Eq. (36) demonstrates that the vacancy generation or annihilation reaction acts to equilibrate $\langle \mu_V \rangle$ to zero, while the migration, dilation, and contraction processes act to equilibrate $\llbracket \mu_V \rrbracket$ to zero. This also implies that if $\llbracket \mu_V \rrbracket \neq 0$, the interface will migrate while the overall system contracts or dilates, and if $\langle \mu_V \rangle \neq 0$ then vacancies will be created or destroyed at the interface.

C. Phenomenological kinetics

Having obtained a thermodynamic description of the generalized solid-solid interface, we present a phenomenological kinetics consistent with Eq. (35). Since the energy must decay under isothermal conditions for spontaneous processes, diffusion and interface motion must occur such that $\dot{\Phi} < 0$. Using this, kinetic expressions can be postulated such that, when inserted into Eq. (35), the overall dissipation rate is negative [5,51,52]. Thus, neglecting cross coupling, the bulk diffusive fluxes are

$$\mathbf{J}_A^\alpha = -m_A^{b,\alpha} \nabla M^\alpha \tag{37}$$

and

$$\mathbf{J}_A^\beta = -m_A^{b,\beta} \nabla M^\beta, \tag{38}$$

where $m_A^{b,\alpha}$ and $m_A^{b,\beta}$ are the bulk diffusive mobilities of atoms in each grain. The adsorption fluxes are

$$q_A^\alpha = -m_A^{t,\alpha}(M^\alpha - M^\Sigma), \tag{39}$$

$$q_A^\beta = -m_A^{t,\beta}(M^\beta - M^\Sigma), \tag{40}$$

where $m_A^{t,\zeta}$ is the mobility of atoms leaving the corresponding bulk grain and adsorbing to the boundary. In the limit of $q_A^\alpha = -q_A^\beta$ and $m_A^{t,\alpha} = m_A^{t,\beta}$, these latter fluxes and mobilities are comparable to transboundary fluxes that have been postulated in other dissipative models of phase transformations [5,51,53–55]. The interface migration rate v_{mgr} is

$$v_{\mathrm{mgr}} = \mathbf{n}^{\alpha\beta} \cdot (\mathbf{v} - \langle \mathbf{u} \rangle) = -L_\Sigma \llbracket \omega \rrbracket, \tag{41}$$

where L_Σ is the interface mobility. Lastly, the relative dilation or contraction rate u_d is

$$u_d = \mathbf{n}^{\alpha\beta} \cdot \llbracket \mathbf{u} \rrbracket = L_d \langle \omega \rangle, \tag{42}$$

where L_d is a kinetic constant for dilation or contraction that indicates how readily lattice sites are incorporated into or removed from a grain. In order to guarantee that the dissipation

rate is negative, the kinetic constants of Eqs. (37)–(42) must all be positive.

III. MODEL FORMULATION

We now formulate a model of the planar grain boundary response under imposed bulk fluxes. Thus, when employing the equations derived in Secs. II B and II C, all instances of Σ are replaced by GB to indicate the corresponding grain boundary quantity. While the same procedure may be employed to obtain a model for the allotropic phase boundary, such a study remains beyond the scope of this work.

For given normal bulk fluxes $J_A^\alpha = \mathbf{n}^{\alpha\beta} \cdot \mathbf{J}_A^\alpha$ and $J_A^\beta = \mathbf{n}^{\alpha\beta} \cdot \mathbf{J}_A^\beta$, we derive expressions for the compositions of the bulk phases and the grain boundary (ρ_A^α, ρ_A^β, and Γ_A). From these compositions, we then obtain expressions for the interface fluxes (q_A^α and q_A^β) and the migration and dilation or contraction rates (v_{mgr} and u_d), and we may also recover the vacancy production rate (H_V^{GB}). The derivation of the model requires the solution of the surface continuity equation [Eq. (13)] for atoms, the interface conditions [Eqs. (29)–(33)], and the phenomenological kinetics [Eqs. (39)–(42)]. From the formulated model, we may then obtain solutions of the system.

We begin with Eq. (13) for Γ_A. Substituting in Eqs. (31)–(33), (39)–(42), and noting that $[\![\rho_0]\!] \equiv 0$ for a grain boundary, we obtain

$$\frac{\partial \Gamma_A}{\partial t} = -q_A^\alpha - q_A^\beta = 2m_A^t(\langle M \rangle - M^{\text{GB}}), \tag{43}$$

where we have made the assumption $m_A^{t,\alpha} = m_A^{t,\beta} = m_A^t$. Two additional equations are available from Eqs. (29) and (30):

$$q_A^\alpha = -J_A^\alpha + \rho_A^\alpha(v - u^\alpha), \tag{44}$$

$$q_A^\beta = J_A^\beta - \rho_A^\beta(v - u^\beta), \tag{45}$$

where $v = \mathbf{n}^{\alpha\beta} \cdot \mathbf{v}$, $u^\alpha = \mathbf{n}^{\alpha\beta} \cdot \mathbf{u}^\alpha$, and $u^\beta = \mathbf{n}^{\alpha\beta} \cdot \mathbf{u}^\beta$ are the normal components of the associated velocities. These are related to v_{mgr} and u_d by

$$v_{\text{mgr}} = v - \frac{u^\alpha + u^\beta}{2}, \tag{46}$$

$$u_d = u^\alpha - u^\beta. \tag{47}$$

We note that, per the model assumptions and definitions in Sec. II, we may choose to define one of v, u^α, or u^β to be zero, fixing the position of either the grain boundary or one outer surface while the remaining domains move in relation to the fixed interface. This is only necessary to recover the individual contributions of v_{mgr} and u_d, but not to derive the overall interface response. Thus, after substituting Eqs. (39), (40), (41), and (42), we obtain

$$J_A^\alpha = m_A^t(M^\alpha - M^{\text{GB}}) - \rho_A^\alpha\left(L_{\text{GB}}[\![\omega]\!] + \frac{L_d}{2}\langle\omega\rangle\right), \tag{48}$$

$$J_A^\beta = -m_A^t(M^\alpha - M^{\text{GB}}) - \rho_A^\beta\left(L_{\text{GB}}[\![\omega]\!] - \frac{L_d}{2}\langle\omega\rangle\right). \tag{49}$$

Equations (43), (48), and (49) are functions of the diffusion potentials and bulk grand potentials, which are functions of the three desired unknowns: ρ_A^α, ρ_A^β,and Γ_A. The model is therefore fully specified when an appropriate free-energy model is provided.

A. Linearized interface response

Due to the strongly nonlinear equations for the concentrations, the model represented by Eqs. (43), (48), and (49) is a coupled, nonlinear set of differential and algebraic equations (DAEs). However, first-order solutions for the compositions at the boundary can be obtained by linearizing the model near equilibrium. We take the Taylor expansion of Eqs. (43), (48), and (49) to first order in ρ_A^α, ρ_A^β and, Γ_A; i.e., an equation F is linearized to first order in the deviation from equilibrium,

$$\bar{F}(\rho_A^\alpha, \rho_A^\beta, \Gamma_A) = F\Big|_{\text{eq}} + \delta_A^\alpha \frac{\partial F}{\partial \rho_A^\alpha}\Big|_{\text{eq}} + \delta_A^\beta \frac{\partial F}{\partial \rho_A^\beta}\Big|_{\text{eq}} + \delta_A^{\text{GB}} \frac{\partial F}{\partial \Gamma_A}\Big|_{\text{eq}} + O(\delta^2), \tag{50}$$

where $\bar{F}$ is the linearized function, $\delta_A^\alpha = \rho_A^\alpha - \rho_A^{\text{eq}}$, $\delta_A^\beta = \rho_A^\beta - \rho_A^{\text{eq}}$, and $\delta_A^{\text{GB}} = \Gamma_A - \Gamma_A^{\text{eq}}$ are the perturbed compositions in the corresponding phases; and ρ_A^{eq} and Γ_A^{eq} are the equilibrium compositions of the corresponding phases. The subscript eq in Eq. (50) indicates that the argument is evaluated at the equilibrium condition given by (ρ_A^{eq}, ρ_A^{eq}, Γ_A^{eq}).

The thermodynamic driving forces must also be linearized to obtain the desired solutions. The bulk diffusion potential and grand potential density are linearized as

$$\bar{M}^b = M^b\Big|_{\text{eq}} + \delta_A^\zeta \frac{\partial M^b}{\partial \rho_A^\zeta}\Big|_{\text{eq}} + O(\delta^2)$$

$$= M^{\text{eq}} + \delta_A^\zeta \frac{\partial^2 f^b}{\partial \rho_A^2}\Big|_{\text{eq}} \tag{51}$$

$$= M^{\text{eq}} + \delta_A^\zeta f_{AA}^b, \tag{52}$$

$$\bar{\omega} = \omega\Big|_{\text{eq}} + \delta_A^\zeta \frac{\partial \omega}{\partial \rho_A^\zeta}\Big|_{\text{eq}} + O(\delta^2)$$

$$= \delta_A^\zeta\left(\frac{\partial f^b}{\partial \rho_A} - M^b - \rho_A \frac{\partial^2 f^b}{\partial \rho_A^2}\right)\Big|_{\text{eq}} \tag{53}$$

$$= -\delta_A^\zeta \rho_A^{\text{eq}} f_{AA}^b, \tag{54}$$

where ζ denotes α or β and

$$f_{AA}^b = \frac{\partial^2 f^b}{\partial \rho_A^2}\Big|_{\text{eq}} \tag{55}$$

is the equilibrium Hessian of the bulk Helmholtz free-energy density. The values of all equilibrium quantities must be the same for α and β at a grain boundary, and therefore we do not include additional superscripts to delineate between the grains. Also, ω^{eq} must be zero in order to satisfy the planar equilibrium condition, and thus it drops out of the linear expression. Likewise, the diffusion potential at the grain boundary is linearized as

$$\bar{M}^{\text{GB}} = M^{\text{GB}}\Big|_{\text{eq}} + \delta_A^{\text{GB}} \frac{\partial M^{\text{GB}}}{\partial \Gamma_A}\Big|_{\text{eq}} + O(\delta^2) = M^{\text{eq}} + \delta_A^{\text{GB}} f_{AA}^{\text{GB}}, \tag{56}$$

where

$$f_{AA}^{\mathrm{GB}} = \left.\frac{\partial^2 f^{\mathrm{GB}}}{\partial \Gamma_A^2}\right|_{\mathrm{eq}} \tag{57}$$

is the Hessian of the excess Helmholtz free-energy density at equilibrium. Both the bulk and grain boundary phases have the same value of M^{eq} for consistency with Eq. (35).

We may now obtain the linearized DAE system. Equations (43), (48), and (49) are linearized according to Eq. (50), which yields

$$\frac{\partial \delta_A^{\mathrm{GB}}}{\partial t} = 2m_A^t\left(\frac{f_{AA}^b}{2}\left(\delta_A^\alpha + \delta_A^\beta\right) - \delta_A^{\mathrm{GB}} f_{AA}^{\mathrm{GB}}\right), \tag{58}$$

$$J_A^\alpha = m_A^t\left(\delta_A^\alpha f_{AA}^b - \delta_A^{\mathrm{GB}} f_{AA}^{\mathrm{GB}}\right) + \left(\rho_A^{\mathrm{eq}}\right)^2 f_{AA}^b\left(L_{\mathrm{GB}}\left(\delta_A^\alpha - \delta_A^\beta\right) + \frac{L_d\left(\delta_A^\alpha + \delta_A^\beta\right)}{4}\right), \tag{59}$$

$$-J_A^\beta = m_A^t\left(\delta_A^\beta f_{AA}^b - \delta_A^{\mathrm{GB}} f_{AA}^{\mathrm{GB}}\right) - \left(\rho_A^{\mathrm{eq}}\right)^2 f_{AA}^b\left(L_{\mathrm{GB}}\left(\delta_A^\alpha - \delta_A^\beta\right) - \frac{L_d\left(\delta_A^\alpha + \delta_A^\beta\right)}{4}\right). \tag{60}$$

The velocities and interface fluxes can then be recovered from the linearized solutions. Here, we take the Taylor expansion of Eqs. (39)–(42) to first order in ρ_A^α, ρ_A^β, and Γ_A. The linearized forms of q_A^α and q_A^β are

$$\bar{q}_A^\alpha = -m_A^t\left(\delta_A^\alpha f_{AA}^b - \delta_A^{\mathrm{GB}} f_{AA}^{\mathrm{GB}}\right), \tag{61}$$

$$\bar{q}_A^\beta = -m_A^t\left(\delta_A^\beta f_{AA}^b - \delta_A^{\mathrm{GB}} f_{AA}^{\mathrm{GB}}\right). \tag{62}$$

Likewise, the linearized forms of v_{mgr} and u_d are

$$\bar{v}_{\mathrm{mgr}} = L_{\mathrm{GB}}\rho_{A,\mathrm{eq}} f_{AA}^b\left(\delta_A^\alpha - \delta_A^\beta\right), \tag{63}$$

$$\bar{u}_d = -\frac{L_d \rho_{A,\mathrm{eq}} f_{AA}^b}{2}\left(\delta_A^\alpha + \delta_A^\beta\right). \tag{64}$$

Collecting Eqs. (58)–(60) and Eqs. (61)–(64), we have a solvable linear index-1 DAE system whose general solution is well posed. A linear ordinary differential equation (ODE) for δ_A^{GB} may be obtained by progressively combining Eqs. (58)–(60) to eliminate δ_A^α and δ_A^β. This yields the linear ODE

$$\frac{\partial \delta_A^{\mathrm{GB}}}{\partial t} = -\frac{2L_d m_A^t f_{AA}^{\mathrm{GB}}\left(\rho_A^{\mathrm{eq}}\right)^2}{2m_A^t + L_d\left(\rho_A^{\mathrm{eq}}\right)^2}\delta_A^{\mathrm{GB}} + \frac{2m_A^t}{2m_A^t + L_d\left(\rho_A^{\mathrm{eq}}\right)^2}[\![J_A]\!]. \tag{65}$$

For an initial value of the perturbation $\delta_{A,0}^{\mathrm{GB}}$, Eq. (65) has the exact solution

$$\delta_A^{\mathrm{GB}}(t) = \delta_{A,SS}^{\mathrm{GB}} + \left(\delta_{A,0}^{\mathrm{GB}} - \delta_{A,SS}^{\mathrm{GB}}\right)\exp\left[-\frac{2L_d m_A^t f_{AA}^{\mathrm{GB}}\left(\rho_A^{\mathrm{eq}}\right)^2}{2m_A^t + L_d\left(\rho_A^{\mathrm{eq}}\right)^2}t\right], \tag{66}$$

where

$$\delta_{A,SS}^{\mathrm{GB}} = \frac{[\![J_A]\!]}{L_d f_{AA}^{\mathrm{GB}}\left(\rho_A^{\mathrm{eq}}\right)^2} \tag{67}$$

is the steady-state solution of the perturbed concentration of atoms in the boundary. Thus, for an initial composition of the grain boundary, a change in $[\![J_A]\!]$ results in an exponential decay to a new steady-state composition. If there is no discontinuity in the bulk flux at the boundary, then atoms will neither accumulate nor deplete in the interface. From either Eqs. (66) or (67), the bulk perturbations and the interfacial velocities and fluxes may be recovered. For brevity, we will only consider the steady-state solutions of the model given by Eq. (67) in the remainder of the work.

B. Free-energy model

To solve the grain boundary response, we must specify the free-energy model of the bulk and the grain boundary. As will be described, we only need the expressions for the diffusion potentials and vacancy chemical potentials. For the bulk, we assume that the solid is an ideal solution of atoms and vacancies, for which the chemical potentials in a bulk grain are

$$\mu_A^b = \mu_A^\ominus + k_B T \ln\frac{\rho_A}{\rho_0}, \tag{68}$$

$$\mu_V^b = \mu_V^\ominus + k_B T \ln\frac{\rho_0 - \rho_A}{\rho_0}, \tag{69}$$

for atoms and vacancies, respectively, where $\mu_A^\ominus$ and $\mu_V^\ominus$ are the corresponding reference chemical potentials and k_B is the Boltzmann constant. The diffusion potential is therefore

$$M^b = \left(\mu_A^\ominus - \mu_V^\ominus\right) + k_B T \ln\frac{\rho_A}{\rho_0 - \rho_A} = M^{\mathrm{eq}} + k_B T \ln\frac{\rho_A\left(\rho_0 - \rho_A^{\mathrm{eq}}\right)}{\rho_A^{\mathrm{eq}}\left(\rho_0 - \rho_A\right)}, \tag{70}$$

where the second equality arises due to the requirement that $M^b = M^{\mathrm{eq}}$ at the equilibrium composition. For the linearized model, the equilibrium value of f_{AA}^b is therefore

$$f_{AA}^b = \frac{k_B T \rho_0}{\rho_A^{\mathrm{eq}}\left(\rho_0 - \rho_A^{\mathrm{eq}}\right)} = \frac{k_B T}{\rho_0 c_A^{\mathrm{eq}}\left(1 - c_A^{\mathrm{eq}}\right)}, \tag{71}$$

where $c_A = \rho_A/\rho_0$ is the site occupancy in the bulk.

For the grain boundary, we assume that the atoms and vacancies form a perfect solution [48,49,56–58]. The corresponding chemical potentials are

$$\mu_A^{\mathrm{GB}} = \mu_A^\ominus - \frac{\gamma - \gamma_A}{\Gamma_0} + k_B T \ln\frac{\Gamma_A}{\Gamma_0}, \tag{72}$$

$$\mu_V^{\mathrm{GB}} = \mu_V^\ominus - \frac{\gamma - \gamma_V}{\Gamma_0} + k_B T \ln\frac{\Gamma_0 - \Gamma_A}{\Gamma_0}, \tag{73}$$

where γ_A and γ_V are the interfacial energies for a system composed entirely of atoms and vacancies, respectively. However, the natural logarithm terms in Eqs. (72) and (73) diverge in these regimes, so the construction of the interface to obtain γ_A and γ_V is purely conceptual. Note that the reference chemical potentials are identical between the bulk and grain boundary phases. The diffusion potential of atoms is therefore

$$M^{\mathrm{GB}} = \left(\mu_A^\ominus - \mu_V^\ominus\right) - \frac{\gamma_V - \gamma_A}{\Gamma_0} + k_B T \ln\frac{\Gamma_A}{\Gamma_0 - \Gamma_A} = M^{\mathrm{eq}} + k_B T \ln\frac{\Gamma_A\left(\Gamma_0 - \Gamma_A^{\mathrm{eq}}\right)}{\Gamma_A^{\mathrm{eq}}\left(\Gamma_0 - \Gamma_A\right)}, \tag{74}$$

where we observe that the dependence upon γ has vanished, and again the second equality arises due to the requirement that $M^{\mathrm{GB}} = M^{\mathrm{eq}}$ at the equilibrium composition. The values of γ_A and γ_V have been absorbed into Γ_A^{eq} and are constant; thus, the equilibrium f_{AA}^{GB} is

$$f_{AA}^{\mathrm{GB}} = \frac{k_B T \Gamma_0}{\Gamma_A^{\mathrm{eq}}\left(\Gamma_0 - \Gamma_A^{\mathrm{eq}}\right)} = \frac{k_B T}{\Gamma_0 \theta_A^{\mathrm{eq}}\left(1 - \theta_A^{\mathrm{eq}}\right)}. \tag{75}$$

Here, $\theta_A = \Gamma_A/\Gamma_0$ is the site occupancy of the grain boundary.

IV. RESULTS AND DISCUSSION

After combining the linearized expressions and constraints from Sec. III A and the expressions for the free energy from Sec. III B, we obtain the steady-state solution for the grain boundary response. The perturbed grain boundary composition is

$$\Gamma_A = \Gamma_A^{\mathrm{eq}} + \frac{\left(1 - \theta_A^{\mathrm{eq}}\right)\theta_A^{\mathrm{eq}}\Gamma_0}{k_B T L_d \left(c_A^{\mathrm{eq}}\rho_0\right)^2}[\![J_A]\!]. \tag{76}$$

The term $1 - \theta_A^{\mathrm{eq}}$ is equivalent to the equilibrium mole fraction of vacancies θ_V^{eq}; similarly, $c_V^{\mathrm{eq}} = 1 - c_A^{\mathrm{eq}}$. At equilibrium, the vacancies are likely very dilute in the metal such that that $c_V^{\mathrm{eq}} \ll 1$ and $\theta_V^{\mathrm{eq}} \ll 1$. In this limit, terms in the linear solution that are proportional to $1 - c_A^{\mathrm{eq}}$ or $1 - \theta_A^{\mathrm{eq}}$ are replaced with c_V^{eq} and θ_V^{eq}, respectively, while terms proportional to c_A^{eq} or θ_A^{eq} may be replaced by one with minimal loss of accuracy. Thus, Eq. (76) becomes

$$\Gamma_A = \Gamma_A^{\mathrm{eq}} + \frac{\theta_V^{\mathrm{eq}}\Gamma_0}{k_B T L_d \rho_0^2}[\![J_A]\!]. \tag{77}$$

We will assume that the vacancies are very dilute in the remainder of the work to simplify the resulting expressions. In Eq. (77), the value of Γ_A diverges if $L_d \to 0$. This is consistent with Eq. (35), as the production or annihilation of lattice sites is required to retain knowledge of $\langle\omega\rangle$ in the overall dissipation. Conversely, Γ_A approaches Γ_A^{eq} as $L_d \to \infty$ since in this limit a local equilibrium exists where the average grand potential is fixed at zero: any necessary lattice site is immediately produced and any excess lattice site is immediately destroyed. It is possible that off-diagonal mobilities for the dissipation terms at the interface may eliminate this divergence, but this is beyond the scope of this study.

From here, we may recover the steady-state solutions for the bulk concentrations on either side of the grain boundary, which are

$$\rho_A^{\alpha} = \rho_A^{\mathrm{eq}} + \frac{c_V^{\mathrm{eq}}}{k_B T \rho_0}\left(\frac{[\![J_A]\!]}{L_d} + \frac{\rho_0^2\langle J_A\rangle}{2L_{\mathrm{GB}}\rho_0^2 + m_A^t}\right), \tag{78}$$

$$\rho_A^{\beta} = \rho_A^{\mathrm{eq}} + \frac{c_V^{\mathrm{eq}}}{k_B T \rho_0}\left(\frac{[\![J_A]\!]}{L_d} - \frac{\rho_0^2\langle J_A\rangle}{2L_{\mathrm{GB}}\rho_0^2 + m_A^t}\right). \tag{79}$$

Equations (78) and (79) also diverge if $L_d \to 0$, which is again consistent with the loss of knowledge of $\langle\omega\rangle$ from the overall energy dissipation rate of the system. Either L_{GB} or m_A^t may be zero, but the solutions diverge if both are zero. Comparing Eqs. (76), (78), and (79), all the atom concentrations of the grain boundary depend upon $[\![J_A]\!]$ and L_d, but only the bulk concentrations at the grain boundary depend upon $\langle J_A\rangle$, L_{GB}, and m_A^t. Therefore, for finite kinetics the surface excess will always be at equilibrium if there is no discontinuity in the bulk flux because the second term of Eq. (76) vanishes when atoms neither accumulate nor deplete at the interface. However, both bulk compositions can have their equilibrium values if and only if both $[\![J_A]\!] = 0$ and $\langle J_A\rangle = 0$ (i.e., the trivial equilibrium solution). As the kinetic constants are all positive, ρ_A^{α} and ρ_A^{β} both shift by the same amount proportional to $[\![J_A]\!]$, but the magnitude of this shift may have a different magnitude than the shift in Γ_A depending on the values of the equilibrium vacancy fractions in all phases.

We now determine the relevant interfacial velocities and fluxes. The migration and dilation or contraction rates are

$$\bar{v}_{\mathrm{mgr}} = \frac{2\rho_0 L_{\mathrm{GB}}\langle J_A\rangle}{2L_{\mathrm{GB}}\rho_0^2 + m_A^t}, \tag{80}$$

$$\bar{u}_d = -\frac{[\![J_A]\!]}{\rho_0}, \tag{81}$$

respectively, where $\bar{u}_d$ has no dependence upon the kinetic constants of the interface as L_d cancels out upon simplification [cf. Eqs. (64), (78), and (79)]. The vacancy generation and annihilation rates and the dilation and contraction rates are related, given by the expression

$$\bar{H}_V^{\mathrm{GB}} = -\rho_0\bar{u}_d = [\![J_A]\!]. \tag{82}$$

As noted in the discussion of Eqs. (46) and (47), we may also recover two of either v, u^{α}, or u^{β} by choosing the GB, S^{α} or S^{β} to have fixed position in the laboratory reference frame. If we choose $u^{\alpha} \equiv 0$ (i.e., S^{α} is fixed), we obtain

$$v = \bar{v}_{\mathrm{mgr}} - \frac{\bar{u}_d}{2} = \frac{4\rho_0^2 L_{\mathrm{GB}} J_A^{\alpha} + m_A^t[\![J_A]\!]}{4L_{\mathrm{GB}}\rho_0^3 + 2\rho_0 m_A^t}, \tag{83}$$

$$u^{\beta} = -\bar{u}_d = \frac{[\![J_A]\!]}{\rho_0} = \frac{\bar{H}_V^{\mathrm{GB}}}{\rho_0}. \tag{84}$$

Thus, in the frame of reference where S^{α} is fixed, the motion of the grain boundary depends upon both $[\![J_A]\!]$ as well as J_A^{α}, but not $\langle J_A\rangle$. Additionally, the relative motion of grain β is a measure of both the dilation and contraction rates and the vacancy production, as the lattice dilates or contracts by the absorption or desorption of vacancies at the grain boundary. Lastly, the values of $\bar{q}_A^{\alpha}$ and $\bar{q}_A^{\beta}$ are equal and opposed,

$$\bar{q}_A^{\alpha} = -\bar{q}_A^{\beta} = -\frac{m_A^t\langle J_A\rangle}{2L_{\mathrm{GB}}\rho_0^2 + m_A^t}, \tag{85}$$

which implies that there is no net absorption of atoms to the interface $q_A^{\mathrm{GB}} = 0$. This is a direct consequence of assuming that the excess surface concentration is at steady state for the given applied flux [cf. Eqs. (65)–(67) and their derivation].

By inspection of Eqs. (76)–(79), we observe that there is a characteristic flux that can be defined for the grain boundary:

$$J^* = k_B T\left[(2L_{\mathrm{GB}} + L_d)\rho_0^2 + m_A^t\right]. \tag{86}$$

This in turn allows us to define dimensionless values of the bulk flux as $\tilde{J}_A^{\alpha} = J_A^{\alpha}/J^*$ and $\tilde{J}_A^{\beta} = J_A^{\beta}/J^*$. Therefore,

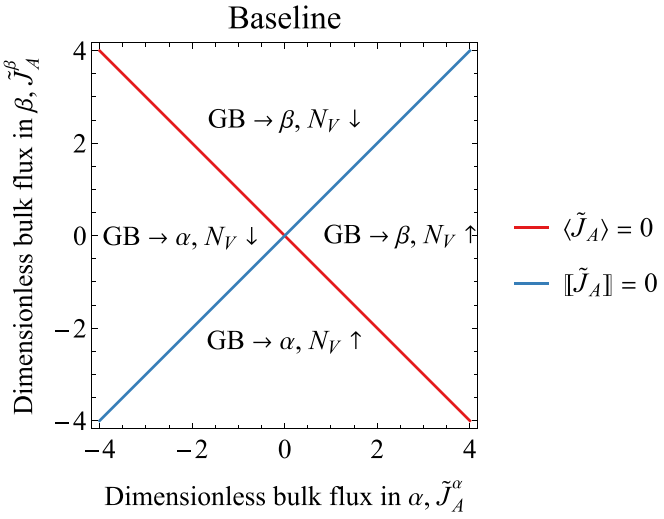

FIG. 3. The interface kinetic response diagram of a grain boundary due to the bulk flux of atoms on either side of the interface, consistent with Eqs. (80)–(82) in the absence of any bounds on the bulk fluxes. In each of the four regions outlined by $\langle\tilde{J}_A\rangle = 0$ and $[\![\tilde{J}_A]\!] = 0$, we indicate whether the grain boundary migrates towards α (GB $\to \alpha$) or β (GB $\to \beta$) and whether the total number of vacancies is increasing ($N_V \uparrow$) or decreasing ($N_V \downarrow$).

Eqs. (76)–(79) may be written in the dimensionless form

$$\theta_A = \theta_A^{\mathrm{eq}} + \theta_V^{\mathrm{eq}} \frac{[\![\tilde{J}_A]\!]}{\tilde{L}_d}, \tag{87}$$

$$c_A^\alpha = c_A^{\mathrm{eq}} + c_V^{\mathrm{eq}} \left(\frac{[\![\tilde{J}_A]\!]}{\tilde{L}_d} + \frac{\langle\tilde{J}_A\rangle}{1-\tilde{L}_d} \right), \tag{88}$$

$$c_A^\beta = c_A^{\mathrm{eq}} + c_V^{\mathrm{eq}} \left(\frac{[\![\tilde{J}_A]\!]}{\tilde{L}_d} - \frac{\langle\tilde{J}_A\rangle}{1-\tilde{L}_d} \right). \tag{89}$$

Here, $\tilde{L}_d = k_B T \rho_0^2 L_d / J^*$ is a dimensionless parameter that indicates whether the grain boundary kinetics is controlled by dilation or contraction and vacancy generation or annihilation ($\tilde{L}_d \to 1$) or migration and transboundary diffusion ($\tilde{L}_d \to 0$). Thus, in this dimensionless space, we can differentiate two vastly different regimes of the grain boundary concentration response. However, in the limit of $\tilde{L}_d \to 0$, we cannot determine whether the resulting behavior is dominated by migration or transboundary diffusion. Given values of $\tilde{L}_d$, θ_A^{eq}, and c_A^{eq}, there are combinations of $[\![\tilde{J}_A]\!]$ and $\langle\tilde{J}_A\rangle$ that will drive one or more of θ_A, c_A^α, and c_A^β to full saturation of atoms (i.e., one) or full depletion of atoms (i.e., zero), which we refer to as critical fluxes. These critical fluxes act to bound the magnitude of the possible interfacial response. In other words, Eqs. (87)–(89) represent an overdetermined system of six implicit equations for $[\![\tilde{J}_A]\!]$ and $\langle\tilde{J}_A\rangle$: the three equations have two solutions for the critical fluxes depending on whether the resulting concentration is equal to zero or one.

A. Graphical interpretation and response under critical fluxes

The behaviors implied by Eqs. (80)–(82) and (87)–(89) can be represented on interface kinetic response diagrams. In Fig. 3, we plot the baseline response of the GB associated with Eqs. (80)–(82) without the constraints implied by the critical fluxes. The axes of the plot are the dimensionless bulk fluxes in each grain, $\tilde{J}_A^\alpha$ and $\tilde{J}_A^\beta$. The red line that starts in the top-left corner and ends in the bottom-right corner indicates that the bulk fluxes are equal and opposed, thus $\langle\tilde{J}_A\rangle = 0$. For the grain boundary, a point along this line corresponds to zero migration [Eq. (80)]. Above and to the right of the red line, $\langle\tilde{J}_A\rangle > 0$, which indicates that the interface will migrate towards the direction of grain β in the sign convention of the model, which is denoted by GB $\to \beta$ in the plot. Below and to the left, $\langle\tilde{J}_A\rangle < 0$, indicating that the interface will migrate towards the direction of grain α, which is denoted by GB $\to \alpha$ in the plot. By comparison, the blue line from the bottom-left corner to the upper-right corner indicates that the bulk fluxes are equal in sign and magnitude, i.e., $[\![\tilde{J}_A]\!] = 0$. This line indicates that the system does not dilate or contract [Eq. (81)]; additionally, vacancies are neither generated nor annihilated [Eq. (82)]. Below and to the right, $[\![\tilde{J}_A]\!] > 0$, and therefore vacancies are generated to counteract the tendency of the interface to become saturated with atoms, which is indicated by $N_V \uparrow$ on the plot (i.e., the total number of vacancies in the system is increased). Simultaneously, according to Eq. (82) the production reaction requires that the system dilates to accommodate the new lattice sites. Above and to the left of the blue line, $[\![\tilde{J}_A]\!] < 0$, and thus the grain boundary is becoming depleted of atoms (i.e., saturated with vacancies) and will annihilate vacancies as a result (indicated by $N_V \downarrow$); the system will contract as these lattice sites are eliminated to decrease the total number of vacancies in the system.

The two dominant modes of the bicrystal evolution are either the migration of the grain boundary from one crystal to another or dilation or contraction of the system; we illustrate these two responses in Fig. 4. If a point is exactly along the blue $[\![\tilde{J}_A]\!] = 0$ line in Fig. 3, then the migration has the apparent effect of one grain growing at the expense of the other. This is demonstrated in Fig. 4(a) for $\langle\tilde{J}_A\rangle > 0$ and 4(b) for $\langle\tilde{J}_A\rangle < 0$. Here, we observe that either grain α grows at the expense of grain β (a) or that grain β grows at the expense of grain α (b), due to the respective sign of $\langle\tilde{J}_A\rangle$. However, the overall system size remains fixed, as the total number of vacancies is conserved. By comparison, if a point is exactly along the red $\langle\tilde{J}_A\rangle = 0$ line in Fig. 3, only a dilation or contraction of the system due to production or annihilation of vacancies will be observed. This is demonstrated in Figs. 4(c) for $[\![\tilde{J}_A]\!] > 0$ (dilation) and 4(d) for $[\![\tilde{J}_A]\!] < 0$ (contraction). The system size is no longer fixed, as the total number of vacancies is nonconserved. The grain boundary will still move with respect to the outer edge of grain α, but the grain boundary velocity must be half of the outer edge of grain β [cf. Eqs. (83) and (84)]. Within the triangular quadrants of Fig. 3 defined by the red and blue lines, both modes are active. The resulting interface motions will be a mixture of the behaviors in Fig. 4.

However, the allowed magnitude of each bulk flux at the grain boundary is finite when we consider the constraining effects of Eqs. (87)–(89), which denote the bounds of $\tilde{J}_A^\alpha$ and $\tilde{J}_A^\beta$ that produce the critical fluxes $\langle\tilde{J}_A\rangle_{\mathrm{crit}}$ and $[\![\tilde{J}_A]\!]_{\mathrm{crit}}$. These implicit bounds are imposed on the interface kinetic response diagrams in Figs. 5(a)–5(c), where the orange lines

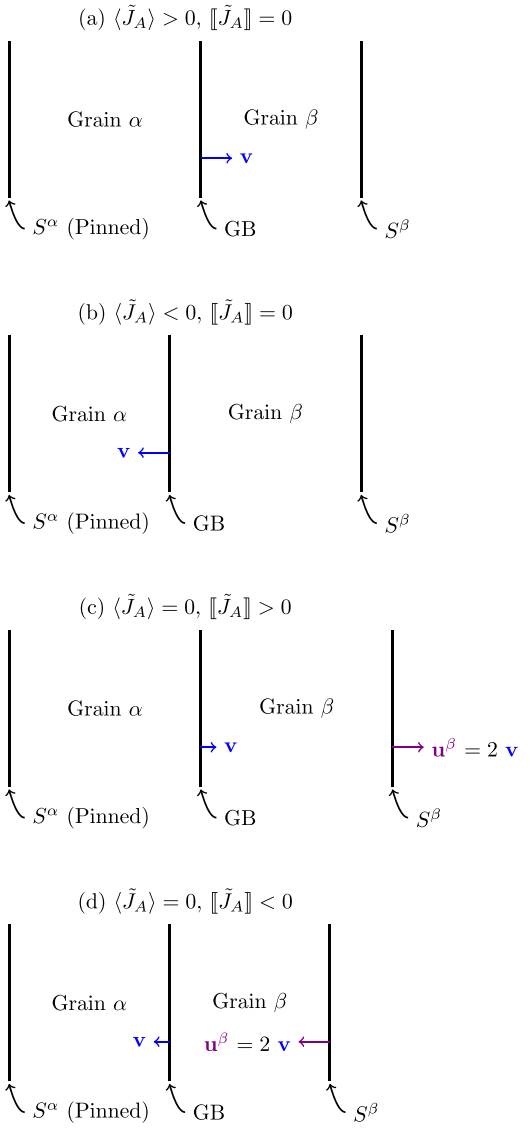

FIG. 4. Schematic of the evolving bicrystal by pure migration (a), (b) and pure dilation or contraction (c), (d) in the reference frame where S^α is pinned. In each panel, the signs of $\langle \tilde{J}_A \rangle$ and $[\![\tilde{J}_A]\!]$ are indicated. Here, the GB always moves, but the total system size is fixed only during migration.

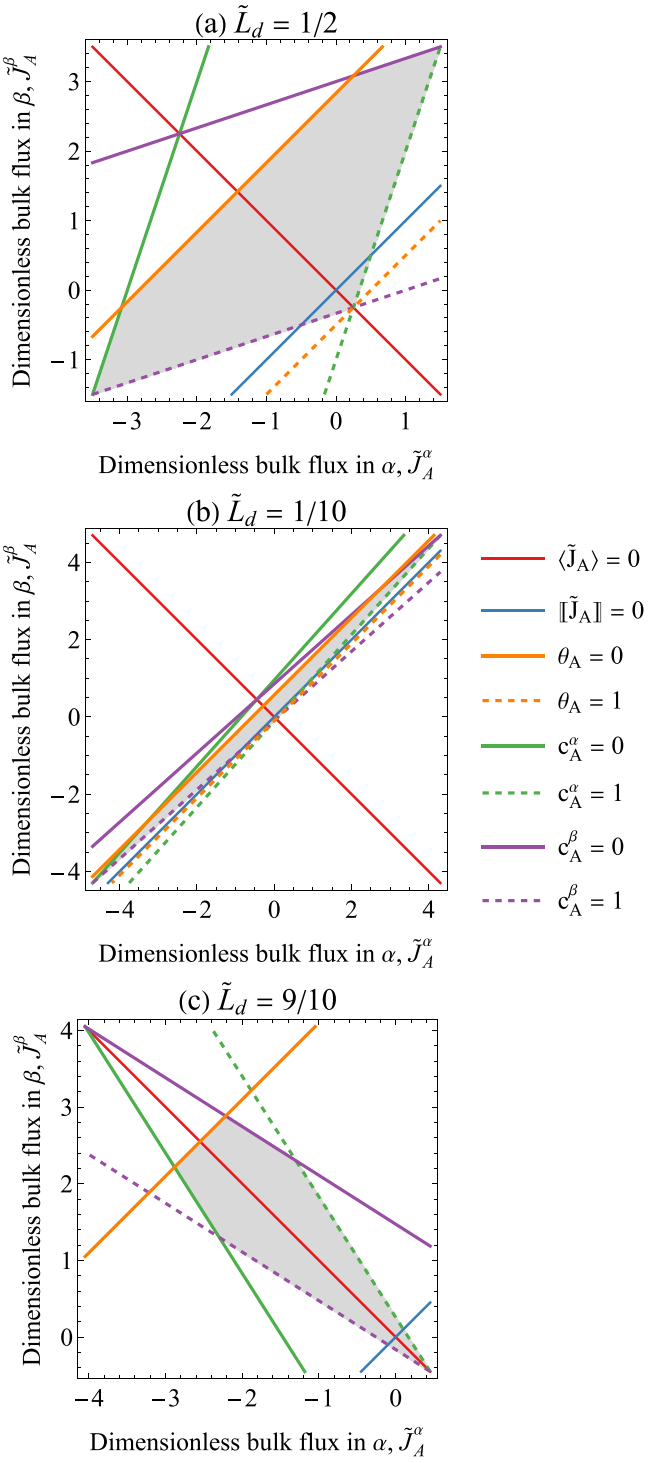

FIG. 5. Constrained interface kinetic response diagrams of a grain boundary due to the bulk flux of atoms on either side of the interface. The two lines for the baseline response (cf. Fig. 3) are marked in each panel. Additionally, we superimpose the six lines defined by Eqs. (87)–(89) that set the critical fluxes for (a) $\tilde{L}_d = \frac{1}{2}$, (b) $\tilde{L}_d = \frac{1}{10}$, and (c) $\tilde{L}_d = \frac{9}{10}$, assuming $c_V^{\rm eq} = 10^{-1}$ and $\theta_V^{\rm eq} = 3c_V^{\rm eq}/2$ for demonstrative purposes. The shaded regions are the portions of the plot that have a valid steady-state solution.

correspond to Eq. (87), the green lines correspond to Eq. (88), and the purple lines correspond to Eq. (89). Additionally, the solid versions of these lines indicate when that portion of the grain boundary is depleted of atoms (saturated with vacancies), and the dashed lines indicate when that portion is saturated with atoms (depleted of vacancies). Here, we assume $c_V^{\rm eq} = 10^{-1}$ and $\theta_V^{\rm eq} = 3c_V^{\rm eq}/2$ for illustrative purposes; more dilute values of the equilibrium vacancy concentration dramatically increase the range of the plots where $\tilde{J}_A^\alpha < 0$ and $\tilde{J}_A^\beta > 0$ and make it difficult to see other regions of the plots. The three plots represent the constrained response of the grain boundary for different values of $\tilde{L}_d$: only pairs of bulk fluxes in the shaded gray regions produce stable steady-state solutions. Bulk fluxes outside the truncated rhomboidal regions that are outlined by the six saturation and depletion lines cannot occur, as one or more concentrations at the interface would be greater than one or less than zero. If we are outside one of the solid

lines that indicates $\theta_A = 0$, $c_A^\alpha = 0$, or $c_A^\beta = 0$, the physical interpretation is that the grain boundary would likely produce pores and voids.

In Fig. 5(a), $\tilde{L}_d = \frac{1}{2}$, indicating balanced contributions from vacancy generation or annihilation and migration or transboundary diffusion. We observe that all three of the dashed saturation lines intersect at the same point on the red line for $\langle \tilde{J}_A \rangle = 0$. The two bulk depletion lines also intersect at a common point on the red line; however, because $\theta_V^{\rm eq} > c_V^{\rm eq}$, the surface depletion line does not pass through this point. If $\theta_V^{\rm eq} = c_V^{\rm eq}$, then all three of the depletion lines would intersect at the same point. The bounds indicated by $\theta_A = 0$ or $\theta_A = 1$ are parallel to the $[\![\tilde{J}_A]\!] = 0$ isoline. Thus, the positive and negative bounds of $[\![\tilde{J}_A]\!]_{\rm crit}$ are uniquely determined by the surface saturation and depletion lines, but the positive bound and negative bound are not equal in magnitude. All three concentrations will saturate at the positive bound of $[\![\tilde{J}_A]\!]_{\rm crit}$, but it is possible for just $\theta_A = 0$ to be satisfied at the negative bound of $[\![\tilde{J}_A]\!]_{\rm crit}$. In contrast, the largest bounds of $\langle \tilde{J}_A \rangle_{\rm crit}$ do not lie along the blue $[\![\tilde{J}_A]\!] = 0$ line. In the upper right, the positive bound of $\langle \tilde{J}_A \rangle_{\rm crit}$ is set by the intersection of the $c_A^\alpha = 1$ and $c_A^\beta = 0$ lines, and in the lower left, the negative bound of $\langle \tilde{J}_A \rangle_{\rm crit}$ is set by the intersection of the $c_A^\alpha = 0$ and $c_A^\beta = 1$ lines. Both bounds are equal in magnitude, unlike $[\![\tilde{J}_A]\!]_{\rm crit}$. If we were to assume $\theta_V^{\rm eq} = 2c_V^{\rm eq}$, the $\theta_A = 0$ constraint would intersect both the positive and negative bounds of $\langle \tilde{J}_A \rangle_{\rm crit}$. In this regime, the allowed region of fluxes would be triangular, and the grain boundary could be saturated with vacancies at any point between $\langle \tilde{J}_A \rangle = 0$ and $\pm\langle \tilde{J}_A \rangle_{\rm crit}$. If we ascribe the $\theta_A = 0$ line to one possible onset of void nucleation, then our interpretation of this result is that increasing the equilibrium vacancy fraction in the grain boundary increases the likelihood of void nucleation.

In Fig. 5(b), $\tilde{L}_d = \frac{1}{10}$, indicating comparatively fast migration or transboundary diffusion kinetics and comparatively slow vacancy generation or annihilation kinetics. The truncated rhomboidal region of allowed bulk fluxes is still present, but the saturation and depletion lines are beginning to flatten out along the $[\![\tilde{J}_A]\!] = 0$ line. As $\tilde{L}_d \to 0$, all the saturation and depletion bounds would collapse onto the blue line, indicating that the grain boundary cannot sustain bulk fluxes such that $[\![\tilde{J}_A]\!] \neq 0$. Thus, any nonzero $[\![\tilde{J}_A]\!]$ should tend to produce voids in this regime. Finally, in Fig. 5(c), $\tilde{L}_d = \frac{9}{10}$, indicating comparatively fast vacancy generation or annihilation kinetics and comparatively slow migration or transboundary diffusion kinetics. Here, the bulk saturation and depletion lines start to approach the $\langle \tilde{J}_A \rangle = 0$ line, and as $\tilde{L}_d \to 1$ then the bulk lines would collapse entirely onto the red line. The grain boundary would then be unable to sustain bulk fluxes such that $\langle \tilde{J}_A \rangle \neq 0$, and a nonzero $\langle \tilde{J}_A \rangle$ would tend to produce voids. Comparing all of Figs. 5(a)–5(c), it is immediately apparent that the allowed region of fluxes where $[\![\tilde{J}_A]\!] > 0$ is much smaller than the region where $[\![\tilde{J}_A]\!] < 0$. Intuitively, this makes sense if vacancies are dilute, very few lattice sites exist in the grain boundary or bulk that can accommodate additional atoms, but many atoms can be removed to produce vacancies.

From the graphical construction of the critical fluxes, we now obtain expressions for the GB response. First, from the intersection of $c_A^\alpha = 1$, $c_A^\beta = 1$, and $\theta_A = 1$, we find

$$\langle J_A \rangle = 0, \tag{90}$$

$$[\![J_A]\!] = J^* [\![\tilde{J}_A]\!] = k_B T \rho_0^2 L_d = H_V^{\rm GB}. \tag{91}$$

By Eqs. (80)–(85), this implies $\bar{v}_{\rm mgr} = 0$ and $\bar{q}_A^\alpha = -\bar{q}_A^\beta = 0$. Further, Eq. (91) is the maximum vacancy production rate and the most positive value of u^β (i.e., the fastest growth rate of the overall bicrystal). Next, we consider the intersection of either $c_A^\alpha = 1$ and $c_A^\beta = 0$ or $c_A^\alpha = 0$ and $c_A^\beta = 1$ (i.e., one bulk grain is entirely composed of vacancies at the boundary), which yields

$$\langle J_A \rangle = J^* \langle \tilde{J}_A \rangle = \pm \frac{k_B T}{2c_V^{\rm eq}} \left(2L_{\rm GB} \rho_0^2 + m_A^t \right), \tag{92}$$

$$[\![J_A]\!] = J^* [\![\tilde{J}_A]\!] = -k_B T \rho_0^2 L_d \frac{1 - 2c_V^{\rm eq}}{2c_V^{\rm eq}} = H_V^{\rm GB}. \tag{93}$$

This combination of fluxes produces the largest magnitudes of $\bar{v}_{\rm mgr}$ and $\bar{q}_A^\alpha = -\bar{q}_A^\beta$, with

$$\bar{v}_{\rm mgr} = \pm \frac{k_B T \rho_0 L_{\rm GB}}{c_V^{\rm eq}}, \tag{94}$$

$$\bar{q}_A^\alpha = \mp \frac{k_B T m_A^t}{2c_V^{\rm eq}}. \tag{95}$$

This regime occurs with significant vacancy annihilation and contraction of the bicrystal. If $\theta_V^{\rm eq} = 2c_V^{\rm eq}$, this is the maximum vacancy annihilation rate. However, if $\theta_V^{\rm eq} = c_V^{\rm eq}$, the maximum vacancy annihilation rate instead occurs at the intersection of $c_A^\alpha = 0$, $c_A^\beta = 0$, and $\theta_A = 0$, which yields

$$\langle J_A \rangle = 0, \tag{96}$$

$$[\![J_A]\!] = J^* [\![\tilde{J}_A]\!] = -k_B T \rho_0^2 L_d \frac{1 - \theta_V^{\rm eq}}{\theta_V^{\rm eq}} = H_V^{\rm GB}. \tag{97}$$

In this regime, the interface is composed entirely of vacancies. Here, the migration rate and transboundary fluxes are again zero, and the contraction rate of the bicrystal is at a maximum. From the constraint equations, we may also determine that $c_V^{\rm eq} \leqslant \theta_V^{\rm eq} \leqslant 2c_V^{\rm eq}$ in order for the present model to be valid. An outcome of this analysis is that the values of $\bar{v}_{\rm mgr}$, $\bar{q}_A^\alpha$, and $H_V^{\rm GB}$ defined from Eqs. (90)–(97) all depend upon the respective kinetic constants $L_{\rm GB}$, m_A^t, and L_d, as do the other quantities related to these first three: $\bar{q}_A^\beta$, $\bar{u}_d$, v, and u^β. The last kinetic constant, L_d, canceled out of Eqs. (80)–(85), which originally suggests an independence of the grain boundary response from L_d. Further, $\bar{v}_{\rm mgr}$ and $\bar{q}_A^\alpha$ are decoupled from each other's kinetic constants, which was not previously the case.

The examination of the critical values of the linearized response of the grain boundary thus has surprising consequences. Whereas the initial steady-state solution given by Eqs. (76)–(85) requires that the kinetic constants be nonzero, Eqs. (90)–(97) remain well posed for zero-valued kinetic constants, provided that the equilibrium vacancy concentrations are nonzero (which is already a requirement of the assumed free-energy model). Thus, the divergence of the steady-state solutions coincides with the magnitudes of the allowed critical fluxes approaching zero. For example, Eqs. (77)–(79)

diverge when $L_d \to 0$, as do Eqs. (87)–(89) when $\tilde{L}_d \to 0$. This implies by necessity that $[\![J_A]\!] \to 0$ (or $[\![\tilde{J}_A]\!] \to 0$); i.e., the grain boundary cannot sustain any discontinuity in the bulk flux without immediately violating the requirement that the site fractions are between zero and one [cf. Fig. 5(b)]. Likewise, the divergence of Eqs. (78) and 79 as both $L_{\mathrm{GB}} \to 0$ and $m_A^t \to 0$ [or Eqs. (88) and (89) as $\tilde{L}_d \to 1$] corresponds to $\langle J_A \rangle \to 0$ (or $\langle \tilde{J}_A \rangle \to 0$). Here, the grain boundary cannot sustain any nonzero average bulk flux without immediately violating the requirement that the site fractions are between zero and one [cf. Fig. 5(c)]. Therefore, although the nucleation process of pores and voids is beyond the scope of this work, we can ascribe the divergence of the steady-state solutions or the vanishing of the allowed fluxes to regimes where such features might begin to form. We note that these results suggest the possibility that pores and voids might form due to either sluggish lattice site annihilation kinetics or sluggish overall atom transport across the grain boundary through a combination of migration and diffusion. Due to the use of linearized kinetics, it is possible that the neglected higher-order terms are significant as the interface fully saturates with or depletes of vacancies. However, the present limits allow an understanding of the basic regimes of the overall theory.

B. Limiting regimes

There are also kinetic regimes of interest that lead to simplifications of Eqs. (76)–(85). First, we consider the combined regimes of local equilibrium and infinitely fast dilation and contraction kinetics, which correspond to $m_A^t \to \infty$ and $L_d \to \infty$, respectively. Taking the respective limits of the analytical solution yields

$$\Gamma_A = \Gamma_A^{\mathrm{eq}}, \tag{98}$$

$$\rho_A^\alpha = \rho_A^\beta = \rho_A^{\mathrm{eq}}, \tag{99}$$

for the interfacial concentrations; i.e., we obtain the expected result that the compositions of the interface are fixed at their equilibrium values. For the migration rate, we obtain

$$\bar{v}_{\mathrm{mgr}} = 0. \tag{100}$$

By comparison, $\bar{H}_V^{\mathrm{GB}}$ and $\bar{u}_d$ have no dependence upon the kinetic parameters of the model and are thus still given by Eqs. (81) and (82), and therefore when grain α is fixed the velocities of the boundary and grain β are

$$v = -\frac{\bar{u}_d}{2} = \frac{[\![J_A]\!]}{2\rho_0} = \frac{\bar{H}_V^{\mathrm{GB}}}{2\rho_0}, \tag{101}$$

$$u^\beta = -\bar{u}_d = \frac{[\![J_A]\!]}{\rho_0} = \frac{\bar{H}_V^{\mathrm{GB}}}{\rho_0}. \tag{102}$$

Equation (100) indicates that, as expected, the planar grain boundary does not migrate when the composition is at local equilibrium [59,60]. However, even though there is no migration of the grain boundary, if $[\![J_A]\!] \neq 0$ such that vacancies are being created or destroyed, then the boundary will move with respect to the edge of grain α at exactly half the rate at which grain β translates. However, this motion is purely due to the dilation or contraction of the grains as vacancies are created or destroyed. The interface fluxes are

$$\bar{q}_A^\alpha = -\bar{q}_A^\beta = -\langle J_A \rangle, \tag{103}$$

which indicates that the interface fluxes are equivalent to the average bulk flux. Therefore, even though we cannot measure either an interface migration rate or a difference in composition at the ideal planar grain boundary, there is still a nonzero flux of atoms across the interface.

Next, we consider the regime where the mobility of the boundary is fast such that $L_{\mathrm{GB}} \to \infty$, as well as infinitely fast dilation and contraction kinetics $L_d \to \infty$. Here, the grain boundary is controlled by the comparatively slow kinetics of transboundary diffusion. The limiting values of the concentrations are

$$\Gamma_A = \Gamma_A^{\mathrm{eq}}, \tag{104}$$

$$\rho_A^\alpha = \rho_A^\beta = \rho_A^{\mathrm{eq}}, \tag{105}$$

which are identical to the local equilibrium case. When we compare both this regime and the fast transboundary diffusion regime to the results of Sec. IV A, both correspond to the $\tilde{L}_d = \frac{1}{2}$ regime [cf. Fig. 5(b)], and therefore their concentration responses are expected to be indistinguishable for given fluxes. As in the local equilibrium regime, $\bar{H}_V^{\mathrm{GB}}$ and $\bar{u}_d$ are given by Eqs. (81) and (82). The limiting value of the migration rate is

$$\bar{v}_{\mathrm{mgr}} = \frac{\langle J_A \rangle}{\rho_0}, \tag{106}$$

and when grain α is fixed, the velocities of the boundary and grain β are

$$v = \bar{v}_{\mathrm{mgr}} - \frac{\bar{u}_d}{2} = \frac{J_A^\alpha}{\rho_0}, \tag{107}$$

$$u^\beta = -\bar{u}_d = \frac{[\![J_A]\!]}{\rho_0} = \frac{\bar{H}_V^{\mathrm{GB}}}{\rho_0}. \tag{108}$$

Therefore, a planar grain boundary in this regime will migrate due to the average bulk flux of atoms, which is distinct from the previous local equilibrium regime despite the identical limit of the compositions. As in the other regimes, the value of u^β only depends upon the value of $[\![J_A]\!]$, but in the fast migration regime, the velocity of the grain boundary only depends upon J_A^α and is not necessarily proportional to u^β. This is also distinct from the local equilibrium regime, and should also allow for this regime to be distinguished from the nonlimiting case. Lastly, the interface fluxes are

$$\bar{q}_A^\alpha = -\bar{q}_A^\beta = 0. \tag{109}$$

In this regime, there is no apparent diffusion of atoms across the planar boundary: all atoms are transferred between grains by the interface migration. However, because $[\![J_A]\!]$ may be nonzero, vacancy generation and annihilation and dilation and contraction can also contribute to the rate at which vacancies, but not atoms, are added to or removed from either grain.

For completeness, we last relax the assumption of $L_d \to \infty$, but maintain either the assumption of $m_A^t \to \infty$ or $L_{\mathrm{GB}} \to \infty$. This corresponds to the $\tilde{L}_d \to 1$ regime in Sec. IV A [cf.

Fig. 5(d)]. Choosing either of the latter assumptions results in the same interface compositions,

$$\Gamma_A = \Gamma_A^{\mathrm{eq}} + \frac{\theta_V^{\mathrm{eq}}\Gamma_0}{k_B T L_d \rho_0^2}[\![J_A]\!], \tag{110}$$

$$\rho_A^{\alpha} = \rho_A^{\beta} = \rho_A^{\mathrm{eq}} + \frac{c_V^{\mathrm{eq}}}{k_B T L_d \rho_0}[\![J_A]\!], \tag{111}$$

which indicate that the interface will either saturate or deplete as a function of the applied flux. The interfacial velocities and fluxes have no dependence upon L_d. Thus, if transboundary diffusion is fast, then $\bar{v}_{\mathrm{mgr}}$, $\bar{q}_A^{\alpha}$, and $\bar{q}_A^{\beta}$ will be given by Eqs. (100) and (103). Otherwise, if migration is fast, then they are given by Eqs. (106) and (109). From the above equations, we conclude that L_d describes the efficiency of the grain boundary as a source or sink of vacancies in the present model, in addition to the kinetics of the dilation and contraction of the overall system. Large values of L_d (fast kinetics) allow the concentrations to approach their equilibrium values, while smaller values (sluggish kinetics) allow for larger deviations from equilibrium.

Overall, the general solution and the limiting regimes suggest that there are a variety of diagnostic conditions that can be considered to assess whether a grain boundary is an ideal source or sink of vacancies:

(1) If the concentration at the grain boundary is not at the expected equilibrium value, then the grain boundary is not an ideal source or sink of vacancies.

(2) If the grain boundary has zero measurable migration, but a nonzero bulk flux exists, then the kinetics of migration are slow in comparison to transboundary diffusion, and local equilibrium may exist.

(3) If a nonzero migration rate can be measured while a nonzero bulk flux exists, then the kinetics of transboundary diffusion may be slow in comparison to the migration.

Regimes 1 (i.e., the general solution) and 3 are key results of the present model that arise from the consideration of vacancy production in the interface, adsorption to the grain boundary, and transboundary diffusion, whereas regime 2 corresponds to traditional definitions of the local equilibrium regime with the explicit addition of vacancy production. Distinguishing among all three regimes should be possible by measuring v and u^{β} in a frame where $u^{\alpha} = 0$ after the grain boundary reaches a steady state for the current values of bulk fluxes. In regime 2, $u^{\beta} = 2v$, indicating fully coupled measurements for any set of bulk fluxes after the interface reaches steady state. Regimes 1 and 3 will have uncoupled measurements of v and u^{β}, but in regime 3 the value of v will not depend upon $[\![J_A]\!]$. As an additional observation, assuming that a given kinetic constant approaches ∞ causes the respective flux expressions given by Eqs. (90)–(97) to also approach ∞. Thus, these idealized kinetic regimes require larger values of either $\langle J_A \rangle$ or $[\![J_A]\!]$ in order to saturate parts of the grain boundary with vacancies, which should act to suppress void formation. In other words, the current analysis suggests that the presence of voids at the grain boundary implies that it is not an ideal source or sink of vacancies and that the processes of migration, transboundary diffusion, and vacancy production and annihilation have finite kinetics.

V. CONCLUSION

By applying the methods of irreversible thermodynamics, we derived the conditions for the motion of a planar grain boundary or allotropic planar phase boundary in a pure metal with vacancies in the stress-free limit. Subsequently, we obtained a linearized analytical solution for the response of the planar grain boundary under imposed bulk fluxes and examined the steady states of this solution for an ideal solution model of atoms and vacancies in the bulk and a perfect solution model in the grain boundary. From this approach, we find the following:

(1) As a consequence of the generalized transport law, a source or sink of vacancies exists at the boundary such that vacancies must be generated or annihilated to equilibrate the interface.

(2) Vacancy generation and annihilation at the boundary are related to the dilation and contraction of the system, respectively, and act to reduce the average bulk grand potential density to zero. Thus, the mass balance conditions and phenomenological kinetics have time-dependent and steady-state solutions.

(3) Away from complete saturation or depletion at the boundary, the migration rate and the transboundary diffusion flux depend upon the average bulk flux, the grain boundary mobility, and transboundary diffusive mobility. However, the vacancy generation and annihilation rates and dilation and contraction rates only depend upon the difference in bulk fluxes across the boundary. Only the surface concentration and the bulk concentrations near the grain boundary depend upon the kinetic parameter for dilation and contraction or, alternatively, the ability of the boundary to absorb or create vacancies.

(4) The allowed values of the bulk fluxes are bounded if any portion of the interfacial region becomes completely saturated with atoms or totally depleted of atoms. In these regimes, the resulting extrema are determined by the kinetic constants for migration, dilation and contraction, and transboundary diffusion, as well as the equilibrium vacancy fractions. It is possible for any or all of the surface and bulk concentrations at the grain boundary to be saturated with vacancies, which suggests the formation of pores and voids can occur either due to sluggish lattice site annihilation or sluggish migration and diffusion across the grain boundary.

(5) For certain combinations of kinetic parameters and bulk fluxes, atoms may transfer from one grain to the other purely by either diffusion or interface migration. If vacancies are created or destroyed, the grains may still grow or shrink as the lattices translate to accommodate the new vacancies, even though the migration rate in the laboratory frame can be zero.

(6) The divergence of the steady-state compositions of the grain boundary coincide with zero values of the bulk fluxes that would tend to saturate or deplete the interfacial region with vacancies. Thus, sluggish interfacial kinetics at the grain boundary should tend to promote the formation of pores and voids in its vicinity. However, an interface with sufficiently fast lattice site generation and annihilation kinetics will be less likely to saturate with vacancies, suppressing the formation of pores and voids. Additionally, this regime will feature local

equilibrium of the diffusion potentials, but not necessarily a zero grand potential.

The expressions derived in this work should be useful in future studies, either for estimating the kinetic parameters of the interface from experiments or for verifying numerical models of vacancy-mediated interface motion.

ACKNOWLEDGMENTS

A.F.C. acknowledges support from the National Science Foundation (NSF) under Award No. DMR-16-11308. The authors also thank D. Dunand at Northwestern University, Y. Mishin at George Mason University, and G. McFadden and W. Boettinger at the National Institutes of Standards and Technology for helpful discussions and comments on this work. This paper was prepared and the accompanying research was performed while A.F.C. was employed at Northwestern University.

The opinions expressed in this article are the author's own and do not necessarily reflect the views of the U.S. Naval Research Laboratory or the United States Government.

APPENDIX A: BALANCE CONDITIONS AT FREE SURFACES

Here, we derive the balance conditions for atoms and vacancies associated with the moving free surface in Sec. II A, following an approach similar to Gurtin and Voorhees [51]. The total number of atoms N_A in the system is

$$N_A = N_A^b + N_A^\Sigma = \int_R \rho_A dV + \int_\Sigma \Gamma_A dA, \tag{A1}$$

where N_A^b and N_A^Σ are the total atoms in the bulk and surface phases, respectively. Likewise, the number of vacancies in the system N_V is

$$N_V = N_V^b + N_V^\Sigma = \int_R \rho_V dV + \int_\Sigma \Gamma_V dA, \tag{A2}$$

where N_V^b and N_V^Σ are the number of vacancies in the respective phases. By Reynolds' theorem, the first variations in time of Eqs. (A1) and (A2) are [41,46]

$$\begin{aligned}\dot{N}_A &= \dot{N}_A^b + \dot{N}_A^\Sigma = \frac{\partial}{\partial t}\int_R \rho_A dV + \frac{\partial}{\partial t}\int_\Sigma \Gamma_A dA \\ &= \int_R \frac{\partial \rho_A}{\partial t} dV + \int_\Sigma \frac{\partial \Gamma_A}{\partial t} dA + \int_\Sigma \rho_A \hat{\mathbf{n}}\cdot\mathbf{v}\, dA,\end{aligned} \tag{A3}$$

$$\begin{aligned}\dot{N}_V &= \dot{N}_V^b + \dot{N}_A^\Sigma = \frac{\partial}{\partial t}\int_R \rho_V dV + \frac{\partial}{\partial t}\int_\Sigma \Gamma_V dA \\ &= \int_R \frac{\partial \rho_V}{\partial t} dV + \int_\Sigma \frac{\partial \Gamma_V}{\partial t} dA + \int_\Sigma \rho_V \hat{\mathbf{n}}\cdot\mathbf{v}\, dA,\end{aligned} \tag{A4}$$

respectively. Both $\partial\rho_A/\partial t$ and $\partial\rho_V/\partial t$ are assumed to obey Eq. (12), and $\partial\Gamma_A/\partial t$ and $\partial\Gamma_V/\partial t$ are assumed to obey Eq. (13). Inserting these expressions, we obtain

$$\dot{N}_A = \int_R \nabla\cdot\mathbf{J}_A^b dV - \int_\Sigma j_A^T dA + \int_\Sigma \rho_A \hat{\mathbf{n}}\cdot\mathbf{v}\, dA \tag{A5}$$

and

$$\dot{N}_V = \int_R \nabla\cdot\mathbf{J}_V^b dV - \int_\Sigma j_V^T dA + \int_\Sigma \rho_V \hat{\mathbf{n}}\cdot\mathbf{v}\, dA. \tag{A6}$$

We now apply the divergence theorem to the bulk to obtain

$$\dot{N}_A = \int_\Sigma \left(\rho_A \hat{\mathbf{n}}\cdot\mathbf{v} - \hat{\mathbf{n}}\cdot\mathbf{J}_A^b - j_A^T\right) dA = 0, \tag{A7}$$

$$\dot{N}_V = \int_\Sigma \left(\rho_V \hat{\mathbf{n}}\cdot\mathbf{v} - \hat{\mathbf{n}}\cdot\mathbf{J}_V^b - j_V^T\right) dA = \int_\Sigma H_V^\Sigma dA, \tag{A8}$$

where the second right-hand sides arise because atoms are conserved in the absence of external sources, but vacancies are not. Here, H_V^Σ is a production or annihilation rate of vacancies at the interface. Equations (A7) and (A8) may be further split into the individual variations from the bulk and surface phases:

$$\dot{N}_A^b = \int_\Sigma q_A^b dA = \int_\Sigma \left(\rho_A \hat{\mathbf{n}}\cdot\mathbf{v} - \hat{\mathbf{n}}\cdot\mathbf{J}_A^b\right) dA, \tag{A9}$$

$$\dot{N}_A^\Sigma = \int_\Sigma q_A^\Sigma dA = -\int_\Sigma j_A^T dA, \tag{A10}$$

$$\dot{N}_V^b = \int_\Sigma q_V^b dA = \int_\Sigma \left(\rho_V \hat{\mathbf{n}}\cdot\mathbf{v} - \hat{\mathbf{n}}\cdot\mathbf{J}_V^b\right) dA, \tag{A11}$$

$$\dot{N}_V^\Sigma = \int_\Sigma q_V^\Sigma dA = -\int_\Sigma j_V^T dA, \tag{A12}$$

where q_A^b, q_A^Σ, q_V^b, and q_V^Σ are fluxes that are positive when atoms or vacancies enter the respective phase, which exist such that Eqs. (A9)–(A12) balance. We may therefore deduce that

$$q_A^b + q_A^\Sigma = 0, \tag{A13}$$

$$q_V^b + q_V^\Sigma = H_V^\Sigma \tag{A14}$$

must be fulfilled to satisfy Eqs. (A7)–(A12). We obtain the mass balance conditions for each species by localizing the surface integrals of Eqs. (A9)–(A12), yielding

$$q_A^b = -\hat{\mathbf{n}}\cdot\mathbf{J}_A^b + \rho_A \hat{\mathbf{n}}\cdot\mathbf{v}, \tag{A15}$$

$$q_A^\Sigma = -j_A^T, \tag{A16}$$

$$q_V^b = -\hat{\mathbf{n}}\cdot\mathbf{J}_V^b + \rho_V \hat{\mathbf{n}}\cdot\mathbf{v}, \tag{A17}$$

$$q_V^\Sigma = -j_V^T. \tag{A18}$$

Combined, Eqs. (A15) and (A16) provide the necessary mass-balance expressions to simplify Eq. (15). Additionally, we have assumed that both ρ_0 and Γ_0 are fixed and that we have a network lattice in the bulk. Therefore, $q_A^\Sigma + q_V^\Sigma = 0$ such that $\partial\Gamma_0/\partial t = 0$, and

$$H_V^\Sigma = \rho_0 \hat{\mathbf{n}}\cdot\mathbf{v} \tag{A19}$$

must be satisfied. Thus, the mass balance conditions dictate that the interface can move only by creating or destroying vacancies.

APPENDIX B: DERIVATION OF GENERALIZED TRANSPORT LAW

Here, we present the particular derivation of the generalized transport law for the system in Sec. II B. These expressions are necessary to obtain both the dissipation rate of the total Helmholtz free energy and the global mass balance conditions. The derivation is generally parallel to that presented by Slattery *et al.* [46] with modifications for the present model's assumptions and notation. We consider the total amount of a quantity in the system Ψ, which has contributions from volumetric densities in R^α and R^β, ψ^α and ψ^β, as well as an excess area density on Σ, ψ^Σ. The total amount is

$$\Psi = \int_{R^\alpha} \psi^\alpha dV + \int_{R^\beta} \psi^\beta dV + \int_\Sigma \psi^\Sigma dA \tag{B1}$$

and the time derivative of Ψ is subsequently

$$\frac{d\Psi}{dt} = \frac{d}{dt}\int_{R^\alpha} \psi^\alpha dV + \frac{d}{dt}\int_{R^\beta} \psi^\beta dV + \frac{d}{dt}\int_\Sigma \psi^\Sigma dA. \tag{B2}$$

We apply Reynolds' theorem to the first two integrals in Eq. (B2):

$$\frac{d}{dt}\int_{R^\alpha} \psi^\alpha dV = \int_{R^\alpha} \frac{\partial \psi^\alpha}{\partial t} dV + \int_\Sigma \psi^\alpha \mathbf{n}^{\alpha\beta}\cdot \mathbf{v}\, dA + \int_{S^\alpha} \psi^\alpha \mathbf{n}^\alpha \cdot \mathbf{u}^\alpha dA, \tag{B3}$$

$$\frac{d}{dt}\int_{R^\beta} \psi^\beta dV = \int_{R^\beta} \frac{\partial \psi^\beta}{\partial t} dV + \int_\Sigma \psi^\beta \mathbf{n}^{\beta\alpha}\cdot \mathbf{v}\, dA + \int_{S^\beta} \psi^\beta \mathbf{n}^\beta \cdot \mathbf{u}^\beta dA, \tag{B4}$$

where $\mathbf{u}^\alpha$ and $\mathbf{u}^\beta$ are the velocities of S^α and S^β, respectively, and $\mathbf{v}$ is the velocity of Σ. By the divergence theorem, we additionally have the identities

$$\int_{R^\alpha} \nabla\cdot(\mathbf{u}^\alpha \psi^\alpha) dV = \int_\Sigma \psi^\alpha \mathbf{n}^{\alpha\beta}\cdot \mathbf{u}^\alpha dA + \int_{S^\alpha} \psi^\alpha \mathbf{n}^\alpha \cdot \mathbf{u}^\alpha dA, \tag{B5}$$

$$\int_{R^\beta} \nabla\cdot(\mathbf{u}^\beta \psi^\beta) dV = \int_\Sigma \psi^\beta \mathbf{n}^{\beta\alpha}\cdot \mathbf{u}^\beta dA + \int_{S^\beta} \psi^\beta \mathbf{n}^\beta \cdot \mathbf{u}^\beta dA. \tag{B6}$$

Note that, due to the absence of elastic deformation and the inclusion of rigid-body motion, $\nabla\cdot\mathbf{u}^\alpha \equiv 0$ and $\nabla\cdot\mathbf{u}^\beta \equiv 0$. Combining Eqs. (B3)–(B6), we obtain

$$\frac{d}{dt}\int_{R^\alpha} \psi^\alpha dV = \int_{R^\alpha} \frac{D\psi^\alpha}{Dt} dV + \int_\Sigma \psi^\alpha \mathbf{n}^{\alpha\beta}\cdot(\mathbf{v}-\mathbf{u}^\alpha) dA, \tag{B7}$$

$$\frac{d}{dt}\int_{R^\beta} \psi^\beta dV = \int_{R^\beta} \frac{D\psi^\beta}{Dt} dV + \int_\Sigma \psi^\beta \mathbf{n}^{\beta\alpha}\cdot(\mathbf{v}-\mathbf{u}^\beta) dA, \tag{B8}$$

where $D\psi^\alpha/Dt = \partial\psi^\alpha/\partial t + \mathbf{u}^\alpha\cdot\nabla\psi^\alpha$ and $D\psi^\beta/Dt = \partial\psi^\beta/\partial t + \mathbf{u}^\beta\cdot\nabla\psi^\beta$ are the material derivatives of ψ^α and ψ^β in the moving reference of the corresponding grain. As we have assumed that Σ is both uniform and planar,

$$\frac{d}{dt}\int_\Sigma \psi^\Sigma dA = \int_\Sigma \frac{\partial \psi^\Sigma}{\partial t} dA. \tag{B9}$$

Inserting Eqs. (B7)–(B9) into (B2), we obtain

$$\frac{d\Psi}{dt} = \int_{R^\alpha} \frac{D\psi^\alpha}{Dt} dV + \int_{R^\beta} \frac{D\psi^\beta}{Dt} dV + \int_\Sigma \frac{\partial \psi^\Sigma}{\partial t} dA + \int_\Sigma \mathbf{n}^{\alpha\beta}\cdot[\![\psi(\mathbf{v}-\mathbf{u})]\!] dA. \tag{B10}$$

This previous equation may be further simplified, yielding the final overall transport law for Ψ:

$$\frac{d\Psi}{dt} = \int_{R^\alpha} \frac{D\psi^\alpha}{Dt} dV + \int_{R^\beta} \frac{D\psi^\beta}{Dt} dV + \int_\Sigma \frac{\partial \psi^\Sigma}{\partial t} dA + \int_\Sigma [\![\psi]\!]\mathbf{n}^{\alpha\beta}\cdot(\mathbf{v}-\langle\mathbf{u}\rangle) dA - \int_\Sigma \langle\psi\rangle \mathbf{n}^{\alpha\beta}\cdot[\![\mathbf{u}]\!] dA. \tag{B11}$$

APPENDIX C: BALANCE CONDITIONS AT SOLID-SOLID INTERFACES

Here, we derive the balance conditions associated with the moving boundary between two grains in Sec. II B, following an approach similar to Gurtin and Voorhees [51] and consistent with Appendixes A and B. The total number of atoms N_A in the system is

$$N_A = N_A^\alpha + N_A^\beta + N_A^\Sigma = \int_{R^\alpha} \rho_A^\alpha dV + \int_{R^\beta} \rho_A^\beta dV + \int_\Sigma \Gamma_A dA, \tag{C1}$$

where N_A^α, N_A^β, and N_A^Σ are the total atoms in the α grain, β grain, and interface, respectively. Likewise, the number of vacancies in the system N_V is

$$N_V = N_V^\alpha + N_V^\beta + N_V^\Sigma = \int_{R^\alpha} \rho_V^\alpha dV + \int_{R^\beta} \rho_V^\beta dV + \int_\Sigma \Gamma_V dA, \tag{C2}$$

where N_V^α, N_V^β, and N_V^Σ are the total vacancies in the α grain, β grain, and interface, respectively. Starting with atoms, the variation in time of Eq. (C1) according to Eq. (B11) is

$$\dot{N}_A = \int_{R^\alpha} \frac{D\rho_A^\alpha}{Dt} dV + \int_{R^\beta} \frac{D\rho_A^\beta}{Dt} dV + \int_\Sigma \frac{\partial \Gamma_A}{\partial t} dA + \int_\Sigma [\![\rho_A]\!]\mathbf{n}^{\alpha\beta}\cdot(\mathbf{v}-\langle\mathbf{u}\rangle) dA - \int_\Sigma \langle\rho_A\rangle \mathbf{n}^{\alpha\beta}\cdot[\![\mathbf{u}]\!] dA. \tag{C3}$$

Inserting the continuity equations (12) and (13), and applying the divergence theorem, the above expression becomes

$$\dot{N}_A = -\int_\Sigma \mathbf{n}^{\alpha\beta}\cdot[\![\mathbf{J}_A^b]\!] dA - \int_\Sigma j_A^T dA + \int_\Sigma [\![\rho_A]\!]\mathbf{n}^{\alpha\beta}\cdot(\mathbf{v}-\langle\mathbf{u}\rangle) dA - \int_\Sigma \langle\rho_A\rangle \mathbf{n}^{\alpha\beta}\cdot[\![\mathbf{u}]\!] dA. \tag{C4}$$

Defining q_A^α, q_A^β, and q_A^Σ as the adsorptive fluxes that add atoms to each region, we additionally have the conditions

$$\dot{N}_A^\alpha = \int_\Sigma q_A^\alpha dA = \int_\Sigma \left[-\mathbf{n}^{\alpha\beta}\cdot\mathbf{J}_A^\alpha + \rho_A^\alpha \mathbf{n}^{\alpha\beta}\cdot(\mathbf{v}-\mathbf{u}^\alpha)\right] dA, \tag{C5}$$

$$\dot{N}_A^\beta = \int_\Sigma q_A^\beta dA = \int_\Sigma \left[\mathbf{n}^{\alpha\beta}\cdot\mathbf{J}_A^\beta - \rho_A^\beta \mathbf{n}^{\alpha\beta}\cdot(\mathbf{v}-\mathbf{u}^\beta)\right]dA, \tag{C6}$$

$$\dot{N}_A^{\mathrm{GB}} = \int_\Sigma q_A^\Sigma dA = -\int_\Sigma j_A^T dA, \tag{C7}$$

where the expressions after the second equality arise from applying Eqs. (B7)–(B9) to N_A^α, N_A^β, and N_A^Σ, and then inserting the associated continuity equations and employing the divergence theorem. If we localize the integrals to the interface, we obtain the one-sided interface conditions for atoms in each region:

$$q_A^\alpha = -\mathbf{n}^{\alpha\beta}\cdot\mathbf{J}_A^\alpha + \rho_A^\alpha \mathbf{n}^{\alpha\beta}\cdot(\mathbf{v}-\mathbf{u}^\alpha), \tag{C8}$$

$$q_A^\beta = \mathbf{n}^{\alpha\beta}\cdot\mathbf{J}_A^\beta - \rho_A^\beta \mathbf{n}^{\alpha\beta}\cdot(\mathbf{v}-\mathbf{u}^\beta), \tag{C9}$$

$$q_A^\Sigma = -j_A^T. \tag{C10}$$

The system is assumed to be closed and isolated, and therefore the atoms are again conserved such that

$$0 = q_A^\alpha + q_A^\beta + q_A^\Sigma = -\mathbf{n}^{\alpha\beta}\cdot[\![\mathbf{J}_A^b]\!] - j_A^T + [\![\rho_A]\!]\mathbf{n}^{\alpha\beta}\cdot(\mathbf{v}-\langle\mathbf{u}\rangle) - \langle\rho_A\rangle\mathbf{n}^{\alpha\beta}\cdot[\![\mathbf{u}]\!] \tag{C11}$$

are the overall conditions dictating the mass balance of atoms.

The derivation of the interface conditions for vacancies is largely identical to the interface conditions for atoms. Therefore, we eventually obtain the one-sided interface conditions

$$q_V^\alpha = -\mathbf{n}^{\alpha\beta}\cdot\mathbf{J}_V^\alpha + \rho_V^\alpha \mathbf{n}^{\alpha\beta}\cdot(\mathbf{v}-\mathbf{u}^\alpha), \tag{C12}$$

$$q_V^\beta = \mathbf{n}^{\alpha\beta}\cdot\mathbf{J}_V^\beta - \rho_V^\beta \mathbf{n}^{\alpha\beta}\cdot(\mathbf{v}-\mathbf{u}^\beta), \tag{C13}$$

$$q_V^\Sigma = -j_V^T, \tag{C14}$$

where q_V^α, q_V^β, and q_V^Σ are the scalar interfacial fluxes of vacancies in each region. As before, vacancies are not necessarily conserved, leading to the overall balance conditions

$$H_V^\Sigma = q_V^\alpha + q_V^\beta + q_V^\Sigma = -\mathbf{n}^{\alpha\beta}\cdot[\![\mathbf{J}_V^b]\!] - j_V^T + [\![\rho_V]\!]\mathbf{n}^{\alpha\beta}\cdot(\mathbf{v}-\langle\mathbf{u}\rangle) - \langle\rho_V\rangle\mathbf{n}^{\alpha\beta}\cdot[\![\mathbf{u}]\!], \tag{C15}$$

where H_V^Σ is the production rate of vacancies in the vicinity of the interface, which is positive when vacancies are generated and negative when vacancies are annihilated. Again, we have assumed fixed ρ_0 and Γ_0 with a network lattice in each grain, such that $q_A^\Sigma + q_V^\Sigma = 0$, and the combination of Eqs. (C11) and (C15) yields

$$H_V^\Sigma = [\![\rho_0]\!]\mathbf{n}^{\alpha\beta}\cdot(\mathbf{v}-\langle\mathbf{u}\rangle) - \langle\rho_0\rangle\mathbf{n}^{\alpha\beta}\cdot[\![\mathbf{u}]\!] \tag{C16}$$

must be satisfied. Thus, as at the free surface, H_V^Σ is related to motion in the system: at a grain boundary, the rate at which the system dilates or contracts can only be nonzero if vacancies are produced or destroyed.

[1] F. R. N. Nabarro, *Theory of Crystal Dislocations*, Dover Books on Physics and Chemistry (Dover, New York, 1987).

[2] C. Herring, Diffusional viscosity of a polycrystalline solid, J. Appl. Phys. **21**, 437 (1950).

[3] R. L. Coble, A model for boundary diffusion controlled creep in polycrystalline materials, J. Appl. Phys. **34**, 1679 (1963).

[4] Y. Mishin, J. A. Warren, R. F. Sekerka, and W. J. Boettinger, Irreversible thermodynamics of creep in crystalline solids, Phys. Rev. B **88**, 184303 (2013).

[5] Y. Mishin, G. B. McFadden, R. F. Sekerka, and W. J. Boettinger, Sharp interface model of creep deformation in crystalline solids, Phys. Rev. B **92**, 064113 (2015).

[6] G. McFadden, W. Boettinger, and Y. Mishin, Effect of vacancy creation and annihilation on grain boundary motion, Acta Mater. **185**, 66 (2020).

[7] J. Svoboda, F. Fischer, and P. Fratzl, Diffusion and creep in multi-component alloys with non-ideal sources and sinks for vacancies, Acta Mater. **54**, 3043 (2006).

[8] F. Fischer, K. Hackl, and J. Svoboda, Improved thermodynamic treatment of vacancy-mediated diffusion and creep, Acta Mater. **108**, 347 (2016).

[9] J. Han, S. L. Thomas, and D. J. Srolovitz, Grain-boundary kinetics: A unified approach, Prog. Mater. Sci. **98**, 386 (2018).

[10] R. L. Coble, Sintering crystalline solids. I. Intermediate and final state diffusion models, J. Appl. Phys. **32**, 787 (1961).

[11] C. Herring, Surface Tension as a Motivation for Sintering, in *The Physics of Powder Metallurgy*, edited by W. Kingston (McGraw-Hill, New York, 1951), pp. 143–179.

[12] Y. Estrin, G. Gottstein, and L. Shvindlerman, Inhibition of void dissolution by vacancies, Scr. Mater. **41**, 415 (1999).

[13] Y. Estrin, G. Gottstein, and L. Shvindlerman, Thermodynamic effects on the kinetics of vacancy-generating processes, Acta Mater. **47**, 3541 (1999).

[14] F. Abdeljawad, D. S. Bolintineanu, A. Cook, H. Brown-Shaklee, C. DiAntonio, D. Kammler, and A. Roach, Sintering processes in direct ink write additive manufacturing: A mesoscopic modeling approach, Acta Mater. **169**, 60 (2019).

[15] I. Greenquist, M. R. Tonks, L. K. Aagesen, and Y. Zhang, Development of a microstructural grand potential-based sintering model, Comput. Mater. Sci. **172**, 109288 (2020).

[16] Y. U. Wang, Computer modeling and simulation of solid-state sintering: A phase field approach, Acta Mater. **54**, 953 (2006).

[17] R. Termuhlen, X. Chatzistavrou, J. D. Nicholas, and H.-C. Yu, Three-dimensional phase field sintering simulations accounting for the rigid-body motion of individual grains, Comput. Mater. Sci. **186**, 109963 (2021).

[18] D. A. Molodov and L. S. Shvindlerman, Interface Migration in Metals (IMM): "Vingt Ans Après" (Twenty Years Later), Int. J. Mater. Res. **100**, 461 (2009).

[19] T. Schuler, P. Bellon, D. R. Trinkle, and R. S. Averback, Modeling the long-term evolution of dilute solid solutions in the presence of vacancy fluxes, Phys. Rev. Mater. **2**, 073605 (2018).

[20] H. R. Peng, M. M. Gong, Y. Z. Chen, and F. Liu, Thermal stability of nanocrystalline materials: Thermodynamics and kinetics, Int. Mater. Rev. **62**, 303 (2017).

[21] P. Lu, F. Abdeljawad, M. Rodriguez, M. Chandross, D. P. Adams, B. L. Boyce, B. G. Clark, and N. Argibay, On the thermal stability and grain boundary segregation in nanocrystalline PtAu alloys, Materialia **6**, 100298 (2019).

[22] A. R. Yost, D. Erdeniz, A. E. Paz y Puente, and D. C. Dunand, Effect of diffusion distance on evolution of Kirkendall pores in titanium-coated nickel wires, Intermetallics **104**, 124 (2019).

[23] T. Hochrainer and A. El-Azab, A sharp interface model for void growth in irradiated materials, Philos. Mag. **95**, 948 (2015).

[24] P. C. Millett, A. El-Azab, S. Rokkam, M. Tonks, and D. Wolf, Phase-field simulation of irradiated metals: Part I: Void kinetics, Comput. Mater. Sci. **50**, 949 (2011).

[25] P. C. Millett, A. El-Azab, and D. Wolf, Phase-field simulation of irradiated metals: Part II: Gas bubble kinetics, Comput. Mater. Sci. **50**, 960 (2011).

[26] A. J. Ardell and P. Bellon, Radiation-induced solute segregation in metallic alloys, Curr. Opin. Solid State Mater. Sci. **20**, 115 (2016).

[27] J. Svoboda and F. Fischer, Incorporation of vacancy generation/annihilation into reactive diffusion concept – Prediction of possible Kirkendall porosity, Comput. Mater. Sci. **127**, 136 (2017).

[28] H.-C. Yu, D.-H. Yeon, A. Van der Ven, and K. Thornton, Substitutional diffusion and Kirkendall effect in binary crystalline solids containing discrete vacancy sources and sinks, Acta Mater. **55**, 6690 (2007).

[29] J. A. Dantzig, W. J. Boettinger, J. A. Warren, G. B. McFadden, S. R. Coriell, and R. F. Sekerka, Numerical modeling of diffusion-induced deformation, Metall. Mater. Trans. A **37**, 2701 (2006).

[30] H.-C. Yu, A. Van der Ven, and K. Thornton, Simulations of the Kirkendall-Effect-Induced deformation of thermodynamically ideal binary diffusion couples with general geometries, Metall. Mater. Trans. A **43**, 3481 (2012).

[31] H.-C. Yu, H.-Y. Chen, and K. Thornton, Extended smoothed boundary method for solving partial differential equations with general boundary conditions on complex boundaries, Modell. Simul. Mater. Sci. Eng. **20**, 075008 (2012).

[32] Y. Estrin and K. Lücke, Grain boundary motion—II. The effect of vacancy production on steady state grain boundary motion, Acta Metall. **29**, 791 (1981).

[33] K. Lücke and G. Gottstein, Grain boundary motion—I. Theory of vacancy production and vacancy drag during grain boundary motion, Acta Metall. **29**, 779 (1981).

[34] M. Upmanyu, D. Srolovitz, L. Shvindlerman, and G. Gottstein, Vacancy generation during grain boundary migration, Interface Sci. **6**, 289 (1998).

[35] P. Cermelli and M. E. Gurtin, The dynamics of solid-solid phase transitions 2. Incoherent interfaces, Arch. Ration. Mech. Anal. **127**, 41 (1994).

[36] T. Frolov, D. L. Olmsted, M. Asta, and Y. Mishin, Structural phase transformations in metallic grain boundaries, Nat. Commun. **4**, 1899 (2013).

[37] F. Larché and J. Cahn, A linear theory of thermochemical equilibrium of solids under stress, Acta Metall. **21**, 1051 (1973).

[38] F. Larché and J. W. Cahn, A nonlinear theory of thermochemical equilibrium of solids under stress, Acta Metall. **26**, 53 (1978).

[39] F. C. Larché and J. W. Cahn, Thermochemical equilibrium of multiphase solids under stress, Acta Metall. **26**, 1579 (1978).

[40] F. Larché and J. Cahn, Overview no. 41 The interactions of composition and stress in crystalline solids, Acta Metall. **33**, 331 (1985).

[41] P. Voorhees and W. C. Johnson, The Thermodynamics of Elastically Stressed Crystals, in *Solid State Physics*, Vol. 59 (Elsevier, Amsterdam, 2004), pp. 1–201.

[42] J.-M. Roussel and P. Bellon, Vacancy-assisted phase separation with asymmetric atomic mobility: Coarsening rates, precipitate composition, and morphology, Phys. Rev. B **63**, 184114 (2001).

[43] K. Ahmed and A. El-Azab, An analysis of two classes of phase field models for void growth and coarsening in irradiated crystalline solids, Mater. Theory **2**, 1 (2018).

[44] Y. Estrin and K. Lücke, Theory of vacancy-controlled grain boundary motion, Acta Metall. **30**, 983 (1982).

[45] R. F. Sekerka, Similarity solutions for a binary diffusion couple with diffusivity and density dependent on composition, Prog. Mater. Sci. **49**, 511 (2004).

[46] J. C. Slattery, L. M. Sagis, and E.-S. Oh, *Interfacial Transport Phenomena*, 2nd ed. (Springer, New York, 2007).

[47] J. Gibbs, in *The Collected Works of J. Willard Gibbs*, edited by W. R. Longley and R. G. Van Name, Vol. 1 (Longmans, Green and Co, New York, 1928).

[48] L. S. Shvindlerman and R. G. Faulkner, Thermodynamics of vacancies and impurities at grain boundaries, Interface Sci. **6**, 213 (1998).

[49] G. Gottstein and L. S. Shvindlerman, *Grain Boundary Migration in Metals: Thermodynamics, Kinetics, Applications*, 2nd ed., CRC Series in Materials Science and Technology (Taylor & Francis, Boca Raton, FL, 2010).

[50] F. Davi and M. E. Gurtin, On the motion of a phase interface by surface diffusion, J. Appl. Math. Phys. **41**, 782 (1990).

[51] M. Gurtin and P. Voorhees, The thermodynamics of evolving interfaces far from equilibrium, Acta Mater. **44**, 235 (1996).

[52] S. R. de Groot and P. Mazur, *Non-Equilibrium Thermodynamics* (Dover, New York, 1984).

[53] M. J. Aziz, Dissipation-theory treatment of the transition from diffusion-controlled to diffusionless solidification, Appl. Phys. Lett. **43**, 552 (1983).

[54] M. Hillert, Solute Drag, Solute trapping and diffusional dissipation of gibbs energy, Acta Mater. **47**, 4481 (1999).

[55] M. Buchmann and M. Rettenmayr, Rapid solidification theory revisited – A consistent model based on a sharp interface, Scr. Mater. **57**, 169 (2007).

[56] C. H. P. Lupis, *Chemical Thermodynamics of Materials* (North-Holland, New York, 1983).

[57] R. Defay and I. Prigogine, Surface tension of regular solutions, Trans. Faraday Soc. **46**, 199 (1950).

[58] D. H. Everett, Thermodynamics of adsorption from solution. Part 1.—Perfect systems, Trans. Faraday Soc. **60**, 1803 (1964).

[59] R. Smoluchowski, Theory of grain boundary motion, Phys. Rev. **83**, 69 (1951).

[60] D. Turnbull, Theory of grain boundary migration rates, JOM **3**, 661 (1951).